KfK 2974
Mai 1980

Isotope Shifts in Unstable Nuclei

Invited Talk Presented at the IOP Conference "Trends in Nuclear Structure Physics" University of Manchester, 16-18 April 1980

H. Rebel
Institut für Angewandte Kernphysik

Kernforschungszentrum Karlsruhe

KERNFORSCHUNGSZENTRUM KARSLRUHE
Institut für Angewandte Kernphysik

KfK 2974

ISOTOPE SHIFTS IN UNSTABLE NUCLEI

Invited Talk presented at the IOP Conference
"Trends in Nuclear Structure Physics"
University of Manchester, 16-18 April 1980

Heinigerd Rebel

Kernforschungszentrum Karlsruhe GmbH, Karlsruhe

Kernforschungszentrum Karlsruhe GmbH
ISSN 0303-4003

Abstract

Current experimental investigations of isotope shifts in atomic spectra of unstable nuclei and the resulting information about size and shape of nuclei far off stability are discussed with reference to some representative examples.

Isotopieverschiebung in atomaren Übergängen instabiler Atomkerne

Experimentelle Untersuchungen der Isotopieverschiebung in radioaktiven Nukliden und die daraus gewonnenen Informationen über Größe und Gestalt der Atomkerne außerhalb des Stabilitätstales werden an Beispielen diskutiert.

1. Introduction

My talk adresses the renewed interest in studies of nuclear structure effects seen in optical spectra of ordinary atoms. Historically, optical spectroscopy is among the oldest experimental techniques in nuclear research and has provided key information on basic quantities of stable and long-lived nuclei through observing hyperfine structure of atomic spectra and isotope shifts of optical lines. Isotope shift refers to small energetic changes in atomic transitions in atoms of fixed atomic number Z and originates from the change in *mass*, in *volume* and *shape* of the nuclei within an isotopic chain.

The richness of information obtainable and the relatively safe theoretical basis have suggested the extension of this way studying nuclei to short-lived nuclei far off stability where the usual balance of nuclear forces has been strongly altered. From experimental point of view this task is primarily a problem of sufficient amount of radioactive material and of the isotopical purity required for samples in classical optical spectroscopy. In recent days we meet this problem in a more favourable situation

- due to efficient mass seperators installed "on line" or "quasi-on-line" at powerful accelerators (example: ISOLDE facility at CERN (see Hansen 1979)) and
- due to the development of quite new spectroscopic methods (Demtröder 1978) which are really fascinating by an impressively high sensitivity and an extremely high spectral resolution, in fact only limited by the natural line width of atomic transitions.

The spectroscopic progress is intimately connected with the application of extraordinary light sources such as narrow banded tunable lasers. Laser techniques have been particularily successful in overcoming the Doppler broadening of spectral lines which is caused by thermal motion of the emitting atoms and often blurs important details in the spectra. The high sensitivity enables an application even in cases where the samples do contain not more than a few hundred atoms. Thus, in recent years, atomic spectroscopy has succeeded in going to "far off stability", and indeed, we have to realize that it provides actually the only practicable experimental method providing information on rms radii of nuclear

charge distributions of unstable nuclei. The already well-known case of the neutron-deficient Hg isotopes (Kühl 1977, Bonn 1972, Huber 1976, Bonn 1976) where unexpected deformation effects have been revealed demonstrates the information potential.* Just those particular findings (fig. 1) may be considered to be the pioneering impact for the revival of atomic spectroscopy in matured days of nuclear physics. Rather than trying to review the present situation in all aspects and to compile results I would like to discuss some particular experiments which represent

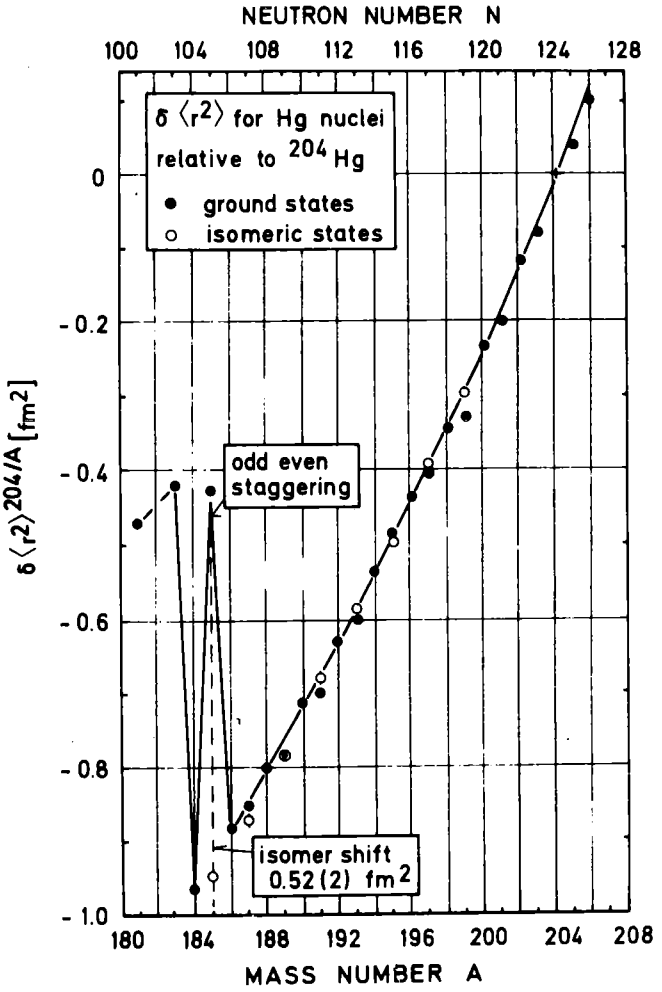

Fig. 1. Changes of nuclear charge radii in Hg as extracted from isotope shift measurements. The jump in the isotope shifts of the light Hg ground states with A ≦ 185 is explained to be due to a sudden on set of strong prolate deformation. The shifts of the even isotopes ^{186,184}Hg follows the slope of the heavier isotopes. Here, the gain in pairing energy favours the oblate deformation (adapted from Kühl et al. 1977).

---

* The present experimental status and systematic features of the Hg radii are briefly given by H.J. Kluge et al. (Kluge et al. 1979).

the present trends and demonstrate the application of various laser spectroscopic methods in isotope shift (IS) and hyperfine-structure splitting (hfs) investigations of short-lived nuclides:

A. SIZE AND SHAPE OF TRANSITIONAL NUCLEI WITH $50 \leq N,Z \leq 82$

a. Atomic-beam-fluorescence-laser spectroscopy of neutron deficient Ba-isotopes (KARLSRUHE: Nowicki et al. 1977, 1978, Bekk et al. 1979)
b. Collinear laser spectroscopy in fast atomic beams of neutron-rich Cs-isotopes (MAINZ: Schinzler et al. 1978, Bonn et al. 1979)
c. On-line-atomic-beam laser spectroscopy of neutron deficient and neutron-rich Cs isotopes (ORSAY: Huber et al. 1978, Liberman et al. 1979)

B. CHARGE RADII OF CA ISOTOPES

Atomic-beam-laser spectroscopy of stable and radioactive Ca-nuclei (HEIDELBERG: Träger et al. 1979 - KARLSRUHE: Andl et al. 1980)

C. DEFORMATION OF FISSION ISOMERS

Isomer shift for the spontaneous fission isomer ^{240m}Am by laser induced nuclear polarization (OAK RIDGE: Bemis et al. 1980)

Before entering the discussions of these examples, for the sake of clarity, we shall first briefly outline the nature of the basic quantities observed in hyperfine structure and isotope shift experiments of that kind.

2. Hyperfine Structure and isotope shift

The schematic level scheme shown in fig. 2 recalls the basic facts of hyperfine structure by looking on the case of the well-known yellow sodium D-lines. Due to the coupling of the spin $\vec{J}$ of the

atomic state with the nuclear spin $\vec{I}$ to the total spin $\vec{F}$ the fine structure is splitted again into several hfs components. In ordinary atoms, hfs splitting is 4 to 6 orders of magnitude smaller than the fine structure splitting. The hfs splitting is primarily due to the interaction of the nuclear moments with the atomic electrons and is determined by two quantities

$$A = \langle I,J,m_I = I,m_J = J|\hat{\mu}\cdot\hat{H}_e|I,J,m_I = I,m_J = J\rangle/(I\cdot J)$$

and

$$B = \langle I,J,m_I = I,m_J = J|\hat{Q}\cdot\hat{\phi}_{ZZ}|I,J,m_I = I,m_J = J\rangle$$

The dipole constant A may be factorized by the magnetic moment μ_I and the magnetic field H_e produced by the valence electrons on the nuclear site

$$A = [\mu_I\cdot H_e(o)/(I\cdot J)]\ (1+\varepsilon)$$

The "hyperfine anomaly" which arises from a nonuniform distribution of nuclear magnetism (Bohr and Weisskopf 1950) over the nuclear volume is taken into account by the hfs anomaly correction ε (<1 %). Though the hyperfine anomaly is itself an interesting nuclear structure effect, up to now only limited information has been obtained from hyperfine anomaly data (Stroke et al. 1961; Moskowitz and Lombardi 1973).
If A and μ_I are known for one stable isotope of a given element the uncertainty in extracting μ_I from the A factor of another isotope is just the differential hfs anomaly.
Similarily, the electric quadrupole constant B may be written as a product

$$B = Q_S\cdot\langle\phi_{ZZ}\rangle_{JJ}$$

by the spectroscopic quadrupole moment $Q_S = \langle\hat{Q}\rangle_{II}$ and the electric field gradient $\langle\phi_{ZZ}\rangle_{JJ}$. A polarization effect (Sternheimer effect) affects the absolute values Q_S deduced (Sternheimer 1950 and 1967). The uncertainties can be minimized when ratios of

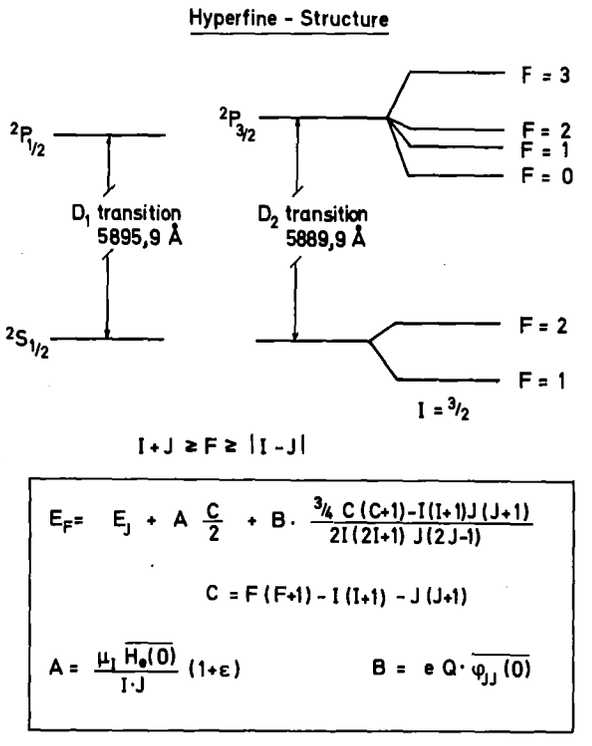

Fig. 2. Hyperfine structure splitting of the Na-D-lines

quadrupole moments are extracted. Note that due to the angular momentum geometry the nuclear quadrupole moment influences only terms with J ≧ 3/2 !
What is the isotope shift?

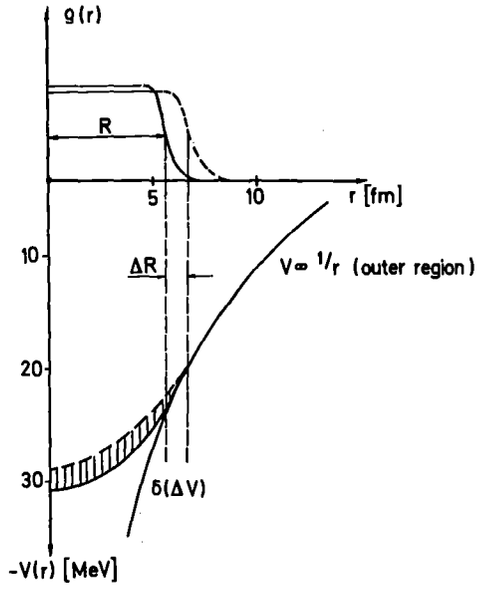

Fig. 3. Volume effect in isotope shift of optical lines

In addition to hyperfine structure we observe small shifts of the centres of gravity of the optical lines of two different isotopes A and A' (even with zero nuclear spin)

$$\delta\nu^{AA'} = \nu^{A'} - \nu^{A} = (\Delta E_F^{AA'} + \Delta E_M^{AA'})/h$$

The contribution of interest for the nuclear physicist is the field (or volume) effect ΔE_F. The finite nuclear size diminishes the binding of the atomic electrons through the overlap of their wave functions with the nuclear volume. The variation of the nuclear radius and of the Coulomb potential in the nuclear interior within an isotopic chain (see fig. 3) influences mainly the s-electrons which are more strongly bound in the smaller isotope.
A second mechanism contributing to the experimentally observed IS originates from the recoil of the electron motion on the nucleus. The mass effect ΔE_M contains a trivial correction due to the different reduced mass of the atom ("normal mass effect") and a contribution depending on the correlation of the electronic momenta ("specific mass effect: $< \sum_{i<j} \vec{p}_i \vec{p}_j >$"). This effect means roughly that mass shift is different for the electrons moving predominantly together as a cluster or distributed randomly around the nucleus. The normal mass effect is dominating in light atoms, but only a few percent in heavier atoms. Both parts of the mass effect are proportional to (A-A')/AA'. As the specific mass effect is very difficult to calculate, especially for complex spectra, it is subject of various uncertainties though there are relatively reliable empirical estimates (Heilig and Steudel 1974). In the analyses of the data we try to rule out the specific mass effect by comparison with sufficiently accurate isotope shift measurements of electronic K_α-X-rays or of muonic X-rays, if available. In the cases of Ba and Cs such a comparison (King-Plot procedure, see Bauche and Champeau 1976) results in a nearly vanishing contribution of the specific mass effect, but with an uncertainty which actually dominates the total uncertainty of the final results of the radius variation. The field shift is determined by the variation $\delta\langle r^2\rangle$ in the nuclear ms charge radii and the change of electron density at the origin. Looking for information on $\delta\langle r^2\rangle$ we need to know the

electronic factor. Alternatively to Hartree-Fock calculations and semiempirical formulas a calibration of optical IS by X-ray-IS measurements in muonic atoms or by electron scattering from stable isotopes is feasible (Stacey 1966).

ELEMENT	Z	$\Delta\nu_{Doppl.}$ (GHz) 200°,500nm	A_S/G_1 (MHz)	$A_{P3/2}/G_1$	$B_{P3/2}/0.1$ barn (MHz)	$IS_{Field}^{A/A+1}/\delta\langle r^2\rangle_{unif}^{A/A+1}$ (MHz)	$IS_{Mass}^{A/A+1}$(500nm) (MHz)
Li	3	3.5	185	1.4	0.5	- 1	6700
Na	11	2.0	600	13	3	- 8	620
K	19	1.5	885	23	6	- 18	210
Rb	37	1.0	1860	46	10	-55	44
Cs	55	0.8	3120	69	13	- 120	18
Hg	80	0.7	34600	424	88	- 4000	8
		$\sim M^{-1/2}$	$\sim Z$	$\sim Z$	$\sim Z$	$\sim Z^2 A^{-1/3}$	$\sim M^{-2}$

Tab. 1. Doppler broadening, expected hyperfine structure and isotope shift in optical lines of various elements

Tab. 1 indicates the experimental conditions and requirements in measuring hfs and IS in atoms of various Z. For observing shifts of about 100 MHz as expected for the field effect of the Cs and Ba resonance lines a sub-Doppler method is obviously necessary.

100 MHz corrsponds to 4.1 x 10^{-7} eV which is in conventional nuclear physics units below the order of pico-MeV. The natural line width is about 10 MHz. Even this number is usually undercut by the instrumental line width of the apparatus used in high-resolution laser spectroscopic experiments.

Experiments going to short-lived nuclides make mostly use of the fact that the nuclides can be provided as a collimated beam which enables a most simple way for reducing the Doppler broading.

The basic set-up of a typical atomic beam laser spectroscopic experiment is the following: Resonance fluorescence of the free atoms is excited in a well-collimated atomic beam by irradiating *transversely* to the beam thus reducing the Doppler broadening. The exciting light source is a narrow band dye laser with fine tuning characteristics, tuned through the resonance. The resonance fluorescence may be observed by a sensitive light detector. There are some modifications of such a scheme, in particular in the method detecting the resonance. the procedure must not use a primarily optical detection method, and indeed there are various sophisticated modications of the basic principle as we will see when considering various examples. The figures of merit in choosing a particular method are sensitivity and peak-to-background ratio.

4. Atomic-Beam-Fluorescence-Laserspectroscopy of Neutron-Deficient Ba-Isotopes

The common nuclear aspect of the experiments performed with Ba- and Cs-nuclides is the transitional behaviour of nuclei found when going away from the magic neutron number N = 82. Transitional nuclei provide a crucial testing ground for nuclear structure models which try to describe the collective degrees of freedom on a phenomenological or microscopic basis. With this point of view the mass region with $50 \leq N,Z < 82$ has been subject of many experimental and theoretical investigations (Sheline et al. 1961, Arseniev et al. 1969). In this corner of the nuclide chart we observe features: level spectra and decay properties which seem to reveal gamma-soft shapes of increasing ms deformation with decreasing neutron number, also indicating a shape transition via the gamma degree of freedom. There is also some evidence for reaching stable deformation far away on the neutron-rich side. The onset of stable deformation is expected around ^{143}Cs (Marshalek et al. 1963).

Triaxiality of the deformation, in particular of the Ba and Xe nuclei is supported not only be the analysis of the even-even nuclei (Habs et al. 1974), but also by the interpretation of the high-spin bands observed in the odd nuclei (Meyer-ter-Vehn 1975). Most extensive theoretical studies of transitional nuclei have been carried out by Kumar and Baranger (1967) on the basis of the pairing-plus-quadrupole model, predicting oblate (disc-shaped) nuclei in the vicinity of ^{126}Ba. This is partly supported by dynamic calculations of collective states of neutron-deficient doubly even Xe and Ba isotopes (Rohozinski et al. 1976). The predicted static quadrupole moments of the 2_1^+ states of the stable nuclides ^{130,134,136,138}Ba may be compared to experimental results extracted from the reorientation effect of Coulomb excitation. Recent results favour negative moments (prolate intrinsic deformation) of the stable even Ba nuclides (Kleinfeld et al. 1977). However, this does not exclude the possibility of oblate shapes in more neutron deficient Ba nuclei and of variations of the deformation from one state to another. In theoretical studies the prolate-oblate groundstate energy differences are quite sensitive to details of the microscopic nuclear structure and to dynamical effects.

As experimental values of rms radii and nuclear moments provide critical tests of the specific ingredients of a particular theoretical approach there is obviously a considerable interest in observing the trends in the rms radii as well as in quadrupole moments or in the deformation effects of the isotope shifts in long isotopic chains.

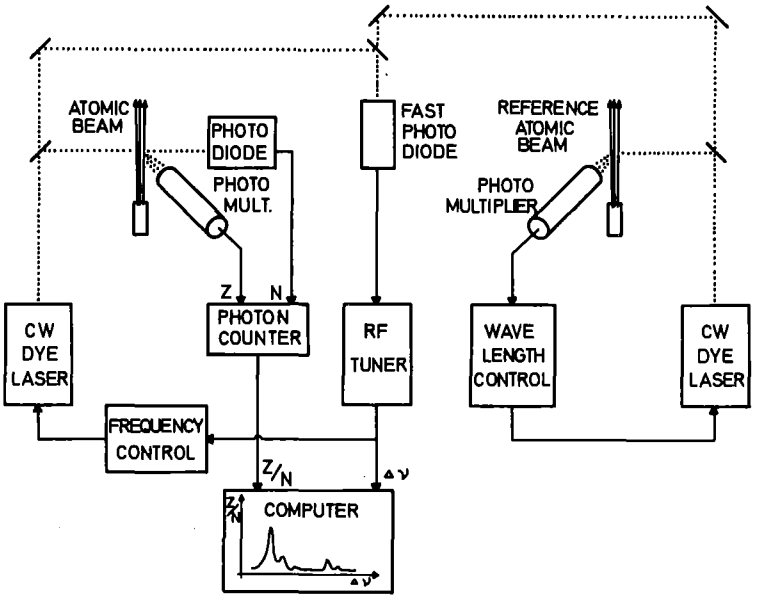

Fig. 4. Schematic view of the experimental set-up used for laser spectroscopic studies of the BaI resonance line in neutron deficient Ba isotopes

The actual setup of the experiments done in KARLSRUHE is schematically shown in Fig. 4 and consists of an apparatus producing a highly collimated beam of radioactive atoms and a second reference beam operated with a stable isotope. The atomic resonance transitions are induced by two tunable high resolution cw dye lasers in single mode operation. One dye laser is locked to the transition frequency of the stable isotope in the reference atomic beam and provides an optical reference frequency. The frequency of the other laser is tuned through the resonance transition and excites fluorescence of the unstable atoms. It is controlled by stabilizing the difference of the two laser frequencies. This is achieved by mixing the light of the two laser beams, on a fast photodiode, the photo current of which is then modulated with the difference frequency, and by comparing this difference frequency with the output signal of a calibrated RF generator. This heterodyne technique enables most precise measurements of optical frequencies. The fluorescence intensity is measured by a single photon counter. Monitoring, data acquisition and control of the experiment are done by a computer interfaced to the experiment by a CAMAC system. Indeed, if really looking in more details the various building blocks appear to be rather complicated devices.

The unstable nuclides have been produced via compound nuclear reactions by charge particle irradiation of appropriate targets at the Karlsruhe Isochronous Cyclotron or by neutron activation in the thermal research Reactor FR2 (Karlsruhe). The production processes are not very isotope selective so that an subsequent enrichment by an electromagnetic mass separator has been necessary. Due to the small shifts and long tails of the Lorentzian line shapes an unambiguous assignment requires the isolation of the interesting isotopes.

Fig. 5 displays one of the more complicated spectra measured for the high spin (11/2) isomer and the groundstate of ^{133}Ba in presence of some impurities of stable barium. The line width is only 10 % larger than the natural line width (19 MHz). This justifies a least-square analysis with pure Lorentzian shapes. But

power broadening (induced emission) and optical pumping have to be avoided. On the other side optical pumping effects provide a useful method identifying the different hyperfine components.

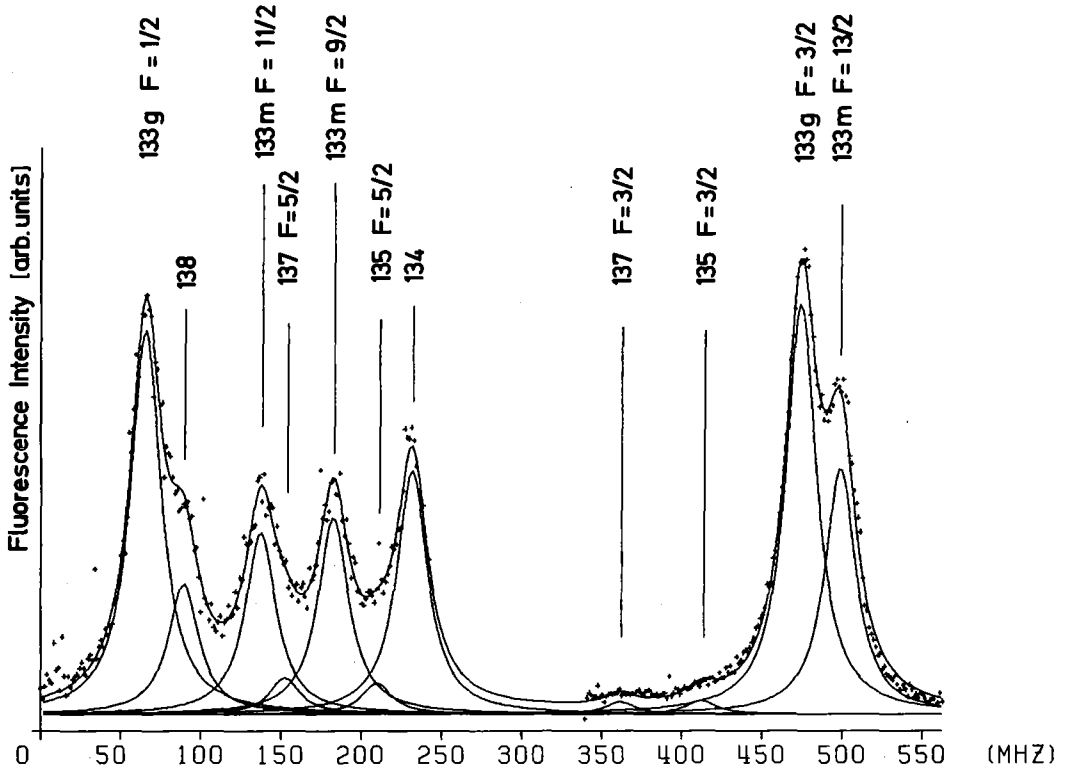

Fig. 5. Fluorescence spectrum of a $^{133m+g}$Ba sample

This feature is schematically indicated in fig. 6 for the case of nuclear spin I = 3/2. It turns out e.g., that exciting the $^1P_1$ hyperfine components by linearily polarized light leads to a saturation of the lowest (F=I-1) component, since only $\Delta m_F=0$ excitations are allowed, spontaneous deexcitation, however, back to all magnetic substates of the groundstate.

As an example, optical pumping effects are shown (fig. 7) in two spectra from a $^{133g+m}$Ba sample, irradiated with linearily polarized light (π light). One component relatively decreases due to

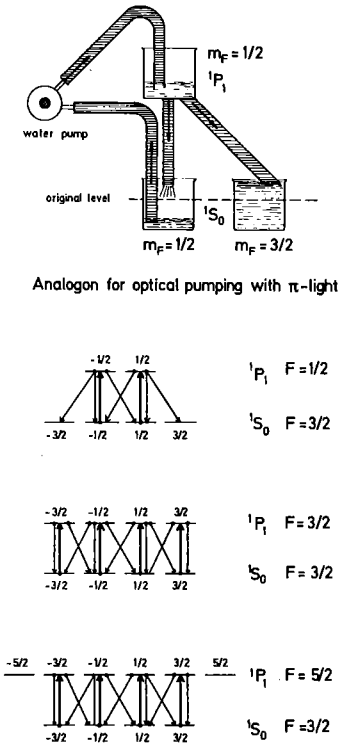

Fig. 6. Optical pumping with linearily polarized (π)-light in a S_0-P_1-transition (I=3/2)

saturation when increasing the laser intensity. It is consequently identified to be the F = 9/2 component in the case of ^{133m}Ba. Please note in the ^{133}Ba spectrum the strong violation of the Landé interval rule, just changing the normal sequence of the hfs components and revealing a large quadrupole moment of the isomeric state. A similar result is present in the case of ^{135m}Ba. The observation of the half-life controls the assignment of a particular isotope. ^{124}Ba has the shortest half life (11.9 min) of all Ba isotopes studied so far. All measurements werde done with a 10 pg sample. In order to value such a number let me mention that the average concentration of Ba in air is about 20 ng/m³ (Vogg and Härtel 1977). From an analysis (Schatz 1979) in view of the probable experimental limits of sensitivity of the measuring method it seems not too optimistic to say that measurements are feasible with 1 pg for even Ba isotopes.

For odd isotopes the above mentioned saturation of the fluorescence intensity prevents increasing the laser intensity and to

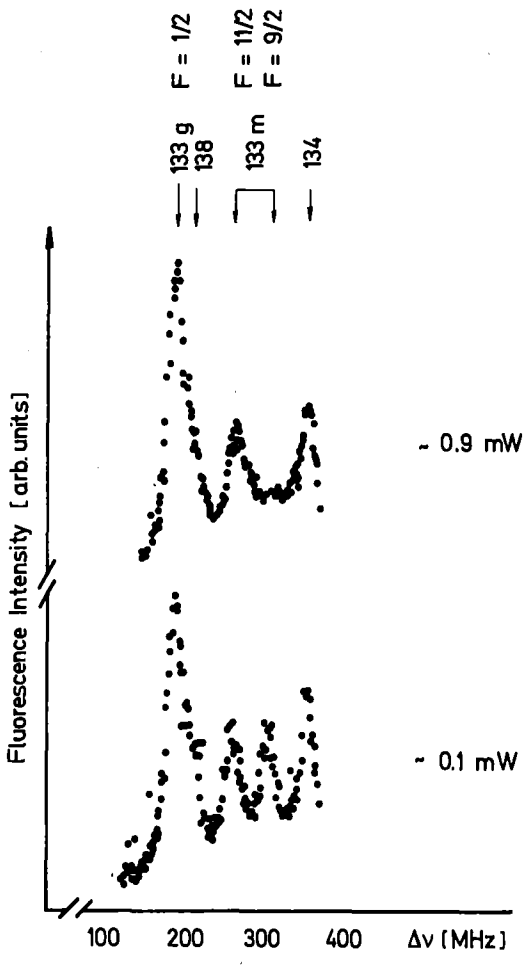

Fig. 7. Parts of two fluorescence spectra taken from a sample of $^{133g+m}$Ba showing optical pumping of the F = 9/2 hfs component when exciting with linearily polarized laser light.

take profit from multiple excitation*. Therefore the sensitivity is about one order of magnitude smaller in the case of odd isotopes unless their spin is 1/2.

The average transit time of a thermal velocity atom passing transversely through the laser beam (1 mm Ø) is about 10^{-5} - 10^{-6} s whereas the lifetime of the excited atomic state is typically in the order of 10^{-8} s. Hence a single atom can be excited repeatedly without considerable power-broadening. Due to the large resonant scattering cross sections ($\sim 10^{-10}$ cm²) and the large photon flux from the lasers it is easy to obtain 10 to 100 scattered photons from each atom during its transit. Greenless et al. have proposed a method which exploits the time correlation of the resonance fluorescence photons for discriminating against random background events. A feature of the photon bursts is a narrowing of the fluo-

* The saturation of particular hfs components can be avoided by use of a fast switcher of the laser light polarization (Nowicki 1980)

rescence line shape. In particular, the wings of the peaks fall off much more rapidly than for a Lorentzian line shape.

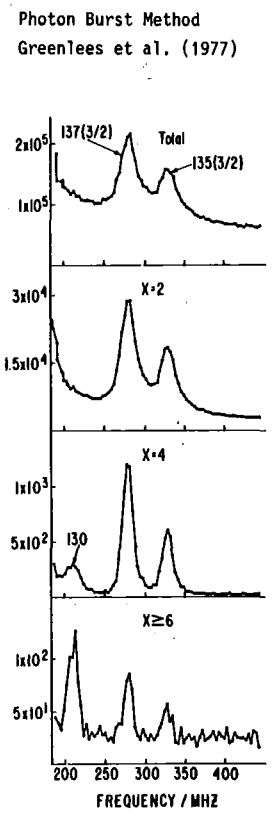

Fig. 8. Parts of fluorescence of natural barium samples (frequencies relative to ^{138}Ba peak) for different multiplicities of the photon bursts (Greenless et al. 1977)

This feature is demonstrated (fig. 8) by comparing the peaks in the spectra of different multiplicities: singles, two-photon events, four-photon-events etc. The probability of detecting several photons per atom falls very quickly with decreasing excitation probability. This might facilitate measurements of small peaks in wings of much larger peaks which is often the experimental situation with radioactive samples and dominating stable impurities. Fig. 9 displays the results of the optical isotope shift measurements after extracting $\delta\langle r^2\rangle$ values. The common systematic uncertainty due to the specific mass shift dominates the overall uncertainty which is indicated by an "error band". Several striking features are evident from the A-dependence:

a. *A prominent odd-even staggering:* in the groundstate the odd nuclei appear to be significantly smaller than the neighbouring even nuclei (negative staggering-values $\gamma_{st} = 2(\langle r^2\rangle_{A+1} - \langle r^2\rangle_A)/(\langle r^2\rangle_{A+2} - \langle r^2\rangle_A)$). The h11/2 isomers,

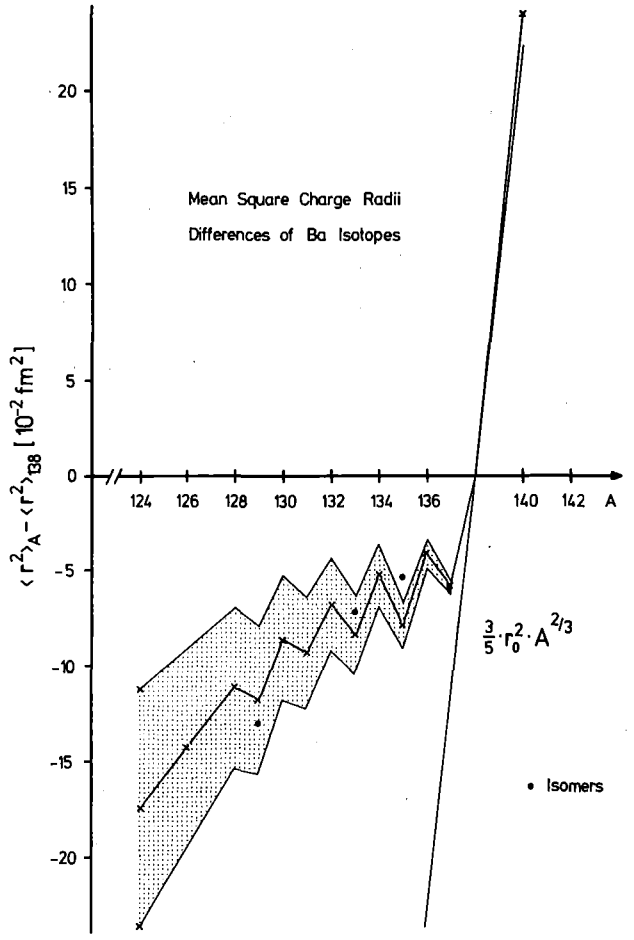

Fig. 9. Differences of ms charge radii of Ba isotopes (Bekk et al. 1979). The straight line represents the A dependence expected for the homogeneous sphere with $R=1.2xA^{1/3}$ fm. The value for ^{140}Ba is deduced from the result of Fischer et al. (1974). According to preliminary results of the Mainz-Isolde collaboration (Mueller 1980) this $\delta\langle r^2\rangle$ value appears to be ca. 10% larger.

however, tend to follow the trend of the even nuclei, in contrast to the g 7/2 isomer of ^{129}Ba.

b. *The overall slope:* with decreasing neutron number the nuclei shrink by far more slowly than expected by the naive liquid drop estimate $\langle r^2\rangle_o \propto A^{2/3}$ (change of ms radius of an incompressible spherical nucleus)

The overall slope can be partly explained by an increasing ms deformation $\langle\beta^2\rangle$ which contributes by a term $\delta\langle r^2\rangle_{Def} = 5/4\pi\langle r^2\rangle_o \delta\langle\beta^2\rangle$. Nuclei which have a nonspherical shape through a permanent or dynamical deformation appear to be more extended radially than spherical nuclei of the same volume. This deformation effect cannot be assumed to be monotonic. Indeed, the odd-even staggering has been qualitively explained by systematic smaller $\delta\langle\beta^2\rangle$-values through a blocking of the groundstate correlations by the odd particle (Reehal and Sorensen 1971). Attributing, however, the

total deviation from the homogeneous sphere-dependence to an increasing deformation on the neutron-deficient side appears to be not consistent with β-values extracted from measured B(E2)-values. The required deformation effect in $\delta\langle r^2\rangle$ is too strong, even if we take into account some uncertainties due to some model-dependence in interpreting B(E2)-values in terms of β. This observation reflects the so-called "isotope shift discrepancy" (Bodmer 1959) which is just due to the change in the monopole part in the measured $\delta\langle r^2\rangle$ accounted by a factor $\eta<1$

$$\delta\langle r^2\rangle = \eta\delta\langle r^2\rangle_o + \frac{5}{4\pi}\langle r^2\rangle_o\delta\langle\beta^2\rangle$$

or by an additional "breathing correction" term $\delta\langle\tilde{r}^2\rangle$

$$\delta\langle r^2\rangle = \delta\langle r^2\rangle_o + \delta\langle\tilde{r}^2\rangle + \frac{5}{4\pi}\langle r^2\rangle_o\delta\langle\beta^2\rangle$$

When neutrons are stripped the charge distribution seems to contract less than it does in the valley of stability, thus suggesting that the nucleus is compressible to some extent and relating the phenomenon to the breathing mode excitations: both features governed by the compressibility of finite nuclear matter.
The "isotope shift anomaly" is an overall feature in all mass regions and should primarily depend on average nuclear properties. This aspect has been discussed by Myers (1969) in the frame work of the droplet model (Myers and Swiatecki 1969, see Myers 1976) which is a refinement of the liquid drop model and takes into account effects associated with deviation of neutron and proton densities from constant bulk values and the difference of the effective boundaries of the neutron and proton distributions. The droplet model with parameters chosen to give the best fit for masses and fission barriers seems to resolve the "isotope shift discrepancy". The good agreement with the experiment is demonstrated in fig. 10 by comparing the inferred experimental deformation (deduced from B(E)-values) with that required by the droplet-model when explaining our data.

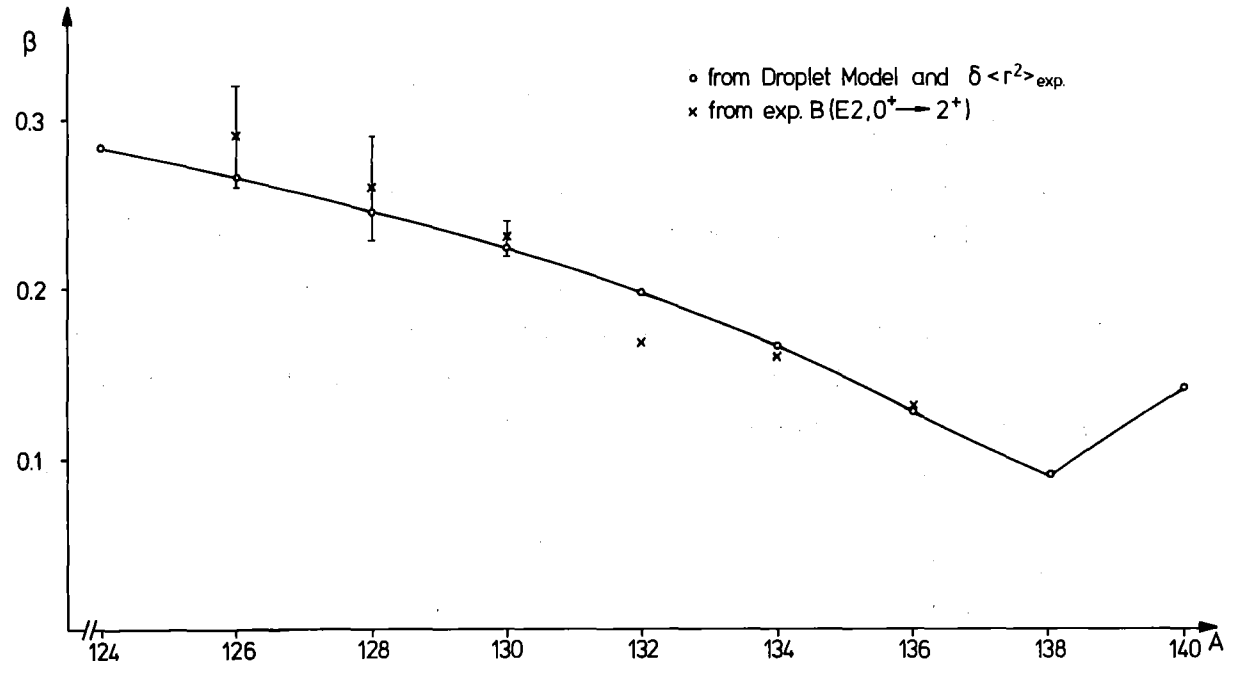

Fig. 10. Deformation of the even Ba isotopes from the droplet model as compared to the results deduced from the B(E2)-values.

The interesting point is that the anomaly in the charge radii appears to be less affected by the value of the nuclear compressibility. The origin of the additional "breathing" $\delta\langle\tilde{r}^2\rangle$ seems to be rather a dilatation caused by the neutron excess, that means by density symmetry term in Myers mass formula. Thus, the phenomenon is related to the question of a "neutron skin" in nuclei (Myers and Swiatecki 1980) and in another language the effect is brought to the dependence of the proton potential on the neutron excess through the isospin dependent part of the nuclear potential (Bohr and Mottelson 1969). This dependence might affect predominantly the diffuse surface region of the real nuclear distribution and give rise to a change of the skin thickness. Indeed when ascribing $\delta\langle\tilde{r}^2\rangle$ to a variation of surface diffuseness a of a Fermi distribution

$$\delta\langle\tilde{r}^2\rangle = \frac{14\pi^2 a^2}{5} \left(\frac{\delta a}{a}\right)$$

relative changes on the order of some percent of the diffuseness parameter a are sufficient to describe the phenomenon (Gerhardt et al. 1979).

c. *Mean-square radii and binding energies:* the sudden increase of the ms charge radius after crossing the closed shells with magic neutron numbers (N=20,28,50 and 52) is associated with a sudden decrease of the binding energies per nucleon. In the vicinity of closed shells the difference $\delta_{A'A}\langle r^2\rangle$ between the ms radii of the isotopes A' and A changes in the opposite sense to the difference $\delta_{A'A}(B/A)$ of the binding energy per nucleon. This empirical statement, recently formulated by Gerstenkorn (1979) is also valid for nuclides with N-4, N-2, N and N+2 neutrons.

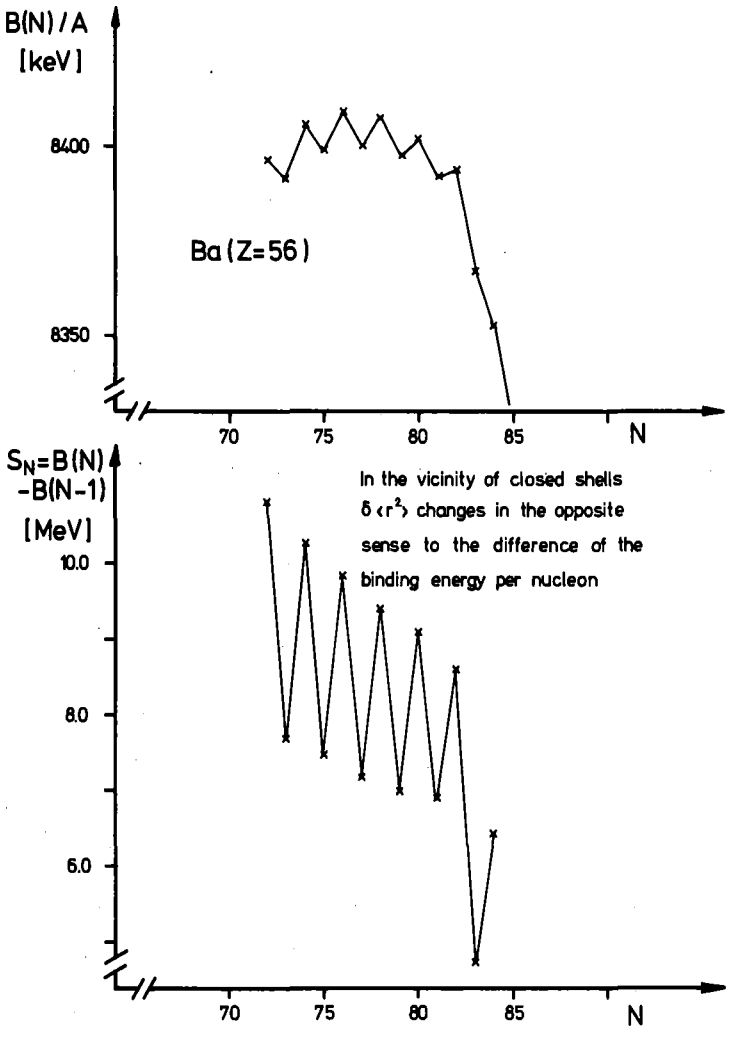

Fig. 11. Variation of binding energies per nucleon and separation energies of Ba isotopes (Wapstra and Bos 1977)

Empirically the relation between overall variations of the binding energies per nucleon and overall variations of the mean square radius appears to be rather simple as long as deformation effects do not interfere (see fig. 11).

In addition to isotopic and isomeric shifts in the ms charge radii the experiments provide information about the electromagnetic moments of the odd nuclei. We do not discuss the results extracted from the measured A and B-factors. But it should be pointed out that a combined consideration of changes in the ms radius and nuclear moments may reveal interesting nuclear structure features, in particular for transitional nuclei. The relatively large quadrupole moments of the isomeric states of ^{135,133,129}Ba, for example (see tab. 2) might mislead us to assume a very large increase in the intrinsic deformation (even a deformation jump in ^{135}Ba). The observed $\delta\langle r^2\rangle$ values, however, are comparatively small and do not allow such an interpretation. This might reflect the more complex relation between quadrupole moments and ms deformation $\langle\beta^2\rangle$ (which represents the sum of the E2 strength (Cline and Flaum 1972)) and is affected by shape fluctuations of transitional nuclei. We have to keep in mind that any interpretation of quadrupole moments in terms of intrinsic deformations invokes a model specifying the possibly complicated intrinsic shape and the type of coupling of the odd particle to the core. In this context a triaxial rotor description has been found to be a better step directed to reality than models restricted to axially symmetric shapes of the nucleus (see Bekk et al. 1979 and references given there). Quite recently Puddu et al. (1980) have shown that the interacting boson model (Arima and Iachello 1975) accounts for the transitional nuclear structure. This is indicated by fig. 12 displaying theoretical and experimental charge radii of neutron-deficient Ce, Ba and Xe nuclides.

A	Q_s eb	$\delta\langle r^2\rangle_{is}$ fm^2	$\delta\langle \beta^2\rangle_{is}$
135 g	0.18 ± 0.02		
m	$1.16 \pm {0.03 \atop 0.02}$	$2.6 \cdot 10^{-2}$	$0.27 \cdot 10^{-2}$
133 g	-		
m	1.08 ± 0.03	$1.2 \cdot 10^{-2}$	$0.13 \cdot 10^{-2}$
129 g	-		
m	1.93 ± 0.03	$-1.2 \cdot 10^{-2}$	$-0.13 \cdot 10^{-2}$

Tab. 2. Comparison of quadrupole moments of the ^{135m,133m,129m}Ba with isomeric shifts in $\delta\langle r^2\rangle$

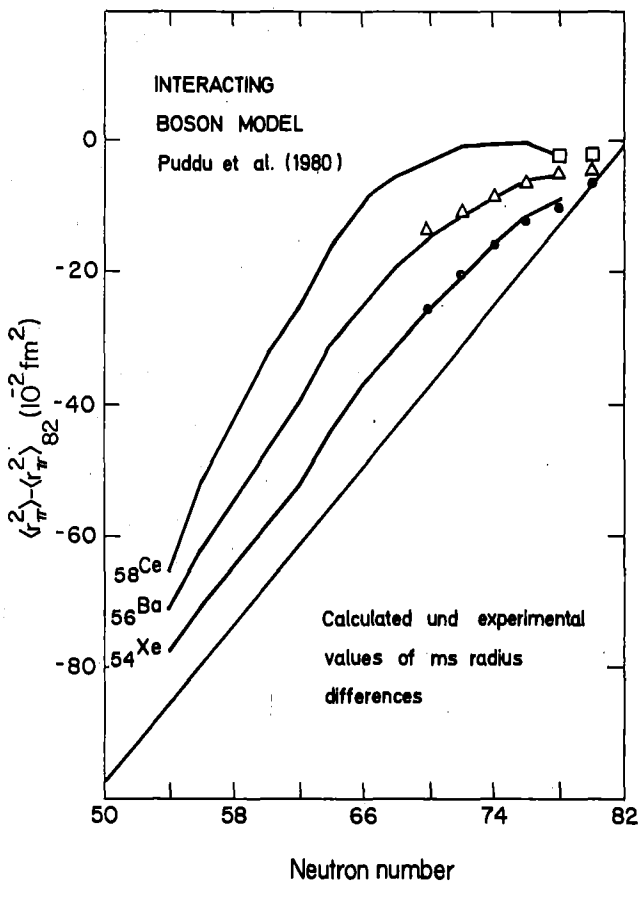

Fig. 12. Experimental rms radii as compared to results from the interacting boson model

5. High-Resolution Laser Spectroscopy in Fast Beams

In order to obtain extremely narrowed optical emission or absorption lines Kaufman (1976) proposed to make use of a velocity bunching phenomenon of fast ions or atoms occurring in the direction of flight.
Consider two identical ions of mass m, having velocity components in beam-direction (Z) of 0 and of thermal velocity $v = (2\ kT/m)^{1/2}$. If both ions are accelerated in this direction through a potential difference U, the final velocities will be,

$$v_a = (2eU/m)^{1/2} \text{ and } v = (v_a^2 + v_o^2)^{1/2} \cong v_a + v_o^2 + v_o^2/2v_a \quad ,$$

respectively. The difference in velocities is reduced, due to the acceleration, by a factor $R = 1/2\ (kT/eU)^{1/2}$. For T = 2000 K and U = 10 kV, $R = 2.1 \times 10^{-3}$. The velocity distribution in the direction perpendicular to the beam axis is, of course, unchanged. The simple explanation of the bunching effect is that ions having a large initial velocity spend less time in the accelerating field and thus gain less velocity than the initially slower ions. If the fast beam is now probed along the beam direction by a parallel monochromatic beam of laser light, the width of an absorption line, neglecting all other sources of broadening, is considerably narrowed. For the resonance transition in neutral cesium (λ = 455.5 nm) e.g. at T = 2000 K and U = 10 kV $\Delta\nu_Z \sim$ 2.3 MHz which is small compared to the natural line width. Of course, the experimental line width obtainable in practice will depend on the angular divergence representing the spread of effective acceleration directions about the beam axis. The absorption can be monitored by observing fluorescence light. Principially, there are two different procedures measuring the hfs structure (see fig. 14), either scanning the laser frequency while keeping the acceleration voltage constant (fixed Doppler shift) or tuning the particle velocity by varying the acceleration voltage keeping the laser frequency constant (Doppler tuning).

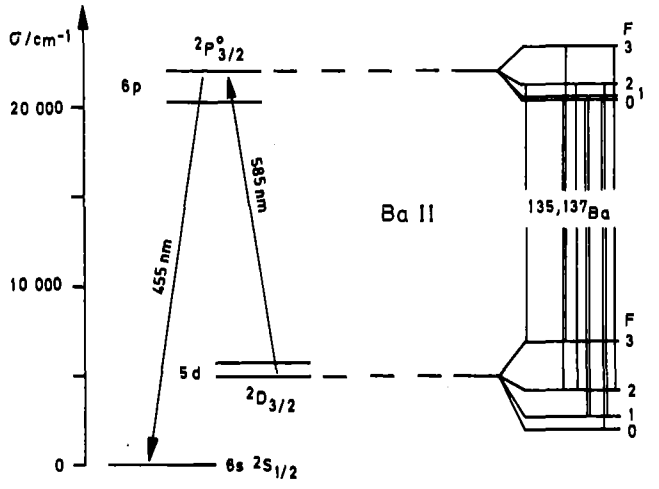

Lowest part of the Ba II level scheme and hyperfine structure splitting of the transition $5d\ ^2D_{3/2} \rightarrow 6p\ ^2P^o_{3/2}$ ($\lambda = 585$ nm) of the odd isotopes ^{135}Ba and ^{137}Ba (both nuclear spin $I = 3/2$)

Fig. 13. Ba II level scheme

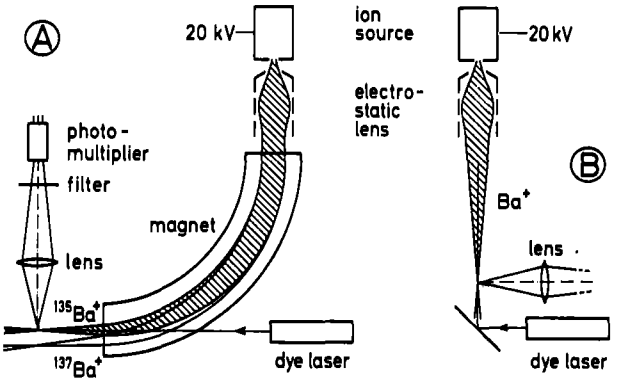

Experimental setup. The Ba ions were investigated by means of a mass separated ion beam with the laser light parallel (downstream) to the ion beam – part A of the figure – or by means of a not separated ion beam with the laser beam antiparallel (upstream) – part B

Fig. 14. Experimental set up in fast beam experiments (Höhle et al. 1978)

The feasibility of the methods has been demonstrated by high resolution experiments with a fast beam of metastable Ba-ions (Höhle et al. 1978). A not-separated (multi mass beam) allows the determination of isotope shifts (the frequency shifts at zero velocity) and atomic masses, as precisely as the beam energy (acceleration voltage) is known.

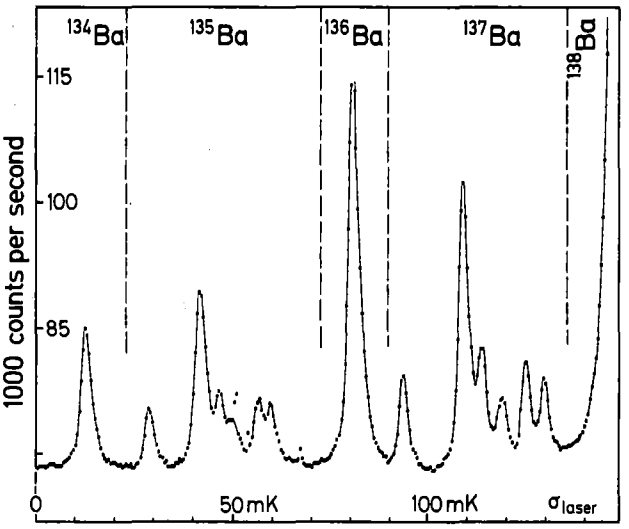

Hyperfine structure of the $5d\ ^2D_{3/2} \rightarrow 6p\ ^2P^o_{3/2}$ transition obtained by monomode laser light absorption from a fast Ba ion beam consisting of all stable Ba isotopes. Due to the different velocities of the isotopes the contributions of the several Ba isotopes to the recorded fluorescence curve are well separated. The rare isotopes ^{130}Ba and ^{132}Ba are out of the region of this laser scan

Fig. 15. Hyperfine structure of the $^2D_{3/2} \rightarrow {}^2P^o_{3/2}$ transition in Ba II measured by fast beam laser spectroscopy (Höhle et al. 1978)

Fig. 15 displays the fluorescence spectrum of a fast Ba ion beam. Due to the different velocities of different isotopes a proper choice of the high voltage separates the contributions of different isotopes very well.

The MAINZ group has combined collinear laser spectroscopy with on-line isotope separation in order to study hfs and isotope shifts of neutron rich Cs isotopes observing the CsI resonance line (Anton et al. 1978, Schinzler et al. 1978, Bonn et al. 1979). The Cs isotopes are produced by fission of ^{235}U at the Mainz TRIGA reactor and prepared as a mass separated beam. The ion beam is neutralized by charge exchange in a Cs vapour cell (fig. 16). The neutralization of the beam is essential as the resonance lines of ions in general are in the UV region inaccessible with single mode lasers presently available.

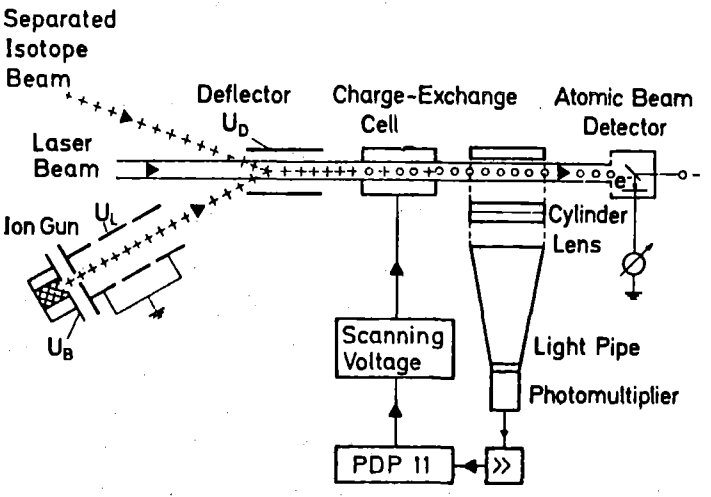

Fig. 16. Scheme of a fast atomic beam on-line experiment investigating neutron rich Cs isotopes (Schinzler et al. 1978)

This charge transfer step may be origin of some difficulties of the method with respect to broadening, deforming and shifting the line profile through charge exchange collisions, possibly obscuring the spectrum analysis and affecting the accuracy. By this method the MAINZ group, however, succeeded to measure hfs splitting and isotope shift of a series of Cs nuclides from ^{137}Cs to ^{142}Cs providing new information on changes of ms radii and on nuclear moments (see fig. 18). By the same method optical isotope shifts and hyperfine structure splitting in fission-produced $^{89-93}Rb$ have been measured (Klempt et al. 1979). Recently fast beam spectroscopy has been adapted to the ISOLDE isotope separator facility and is going to start measurements of isotope shifts and hfs in neutron rich Ba nuclei (Mueller 1980).

6. On-line Atomic-Beam Laser Spectroscopy of Neutron Deficient and Neutron Rich Cs Isotopes

The first successful on-line laser spectroscopic measurements were performed by a group of ORSAY studying short-lived sodium isotopes ($^{21-25}$Na) by use of an interesting combination of atomic-beam laser spectroscopy and optical pumping techniques (Huber et al. 1975). More recently (Huber et al. 1978) the method, somewhat refined and modified, has been applied to hfs and IS studies of neutron deficient Cs isotopes ($^{121-137}$Cs), which have been produced by spallation of lanthanum and separated in mass by the ISOLDE on-line facility. Fig. 17 explains the principles of the experimental configuration. The separated isotopes are transformed into a sufficiently collimated atomic beam and pass a sixpole magnet which focusses atoms with the atomic spin polarisation $m_j = + 1/2$ into the opening of a surface ionizer of a mass separator. Atoms with $m_j = - 1/2$ are defocussed.

Even though mass separation of radioactive nuclei is already achieved by Isolde, for a sensitive detection of the focussed atoms of interest a mass spectrometer is necessary in order to eliminate the high background of stable isotopes.

Before entering the state selecting sixpole magnet optical transitions between the hfs components of the D lines are selectively induced by a tunable narrow-banded dye laser. After each excitation (say, $^2S_{1/2}$ (F = I-1/2) $\rightarrow$ $^2P_{1/2}$) a certain fraction of atoms is falling back into the other not absorbing component of the ground-state ($^2S_{1/2}$ (F = I+1/2)). All of them will finally be pumped into this state. Thus this hyperfine optical pumping changes the population distribution between the hyperfine components of the ground-state. After having entered adiabatically the strong Paschen-Back field of the sixpole, however, all sublevels of the F = I-1/2 are transformed into the $m_j = - 1/2$ substates whereas those of the F = I+1/2 have run into the $m_j = + 1/2$ components. One observes an increase of the beam intensity when pumping into the F = I+1/2 ground state and a decrease when pumping into the F = I-1/2 level. For purpose of calibration a scan of a stable reference isotope can be obtained by measuring the fluorescence from a separate atomic beam.

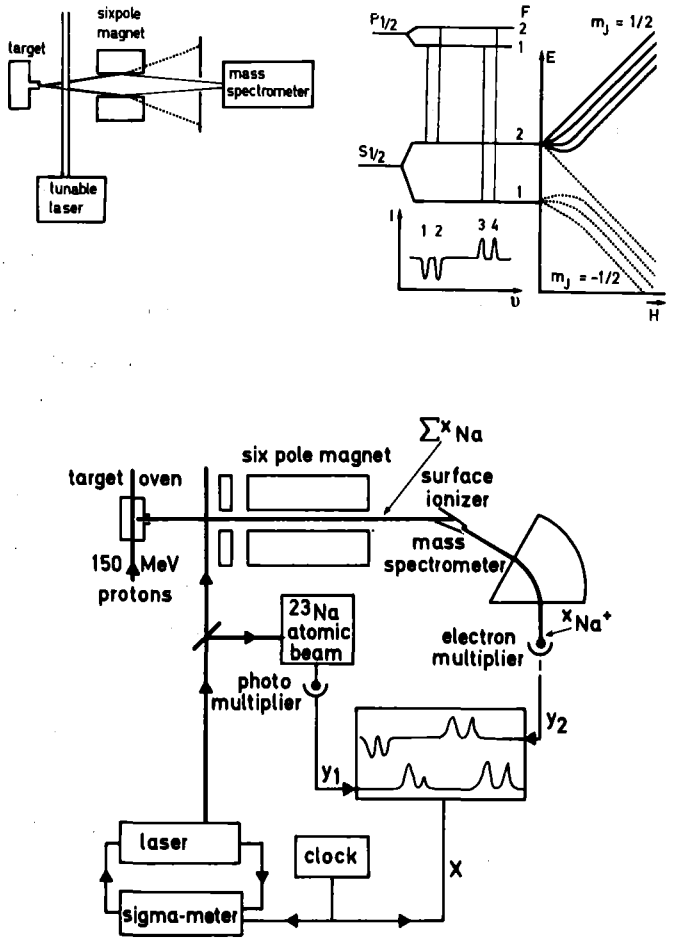

Fig. 17. Principle of the on-line laser spectroscopic experiments of the Orsay group (Huber et al. 1975)

This non-optical detection is characterized by an ultimate efficiency and very low background*. Compared to optical detection, the signal-to-background ratio is considerably increased up to a factor of 10^3.

In most recent experiments based on this method (Liberman et al. 1979) isotope shifts and hyperfine structure splitting of the D_2 lines have been measured for a long chain of isotopes ranging from ^{137}Cs with magic neutron number to ^{121}Cs, and for several isomers. The extremely small changes of the rms radii just below N = 82 had been known from standard optical spectroscopy on stable and

*A special application of this combination of atomic beam and laser techniques has recently permitted the first observation of an optical transition in francium (Z = 87), the D_2 line at 717.7 nm (Liberman et al. 1978)

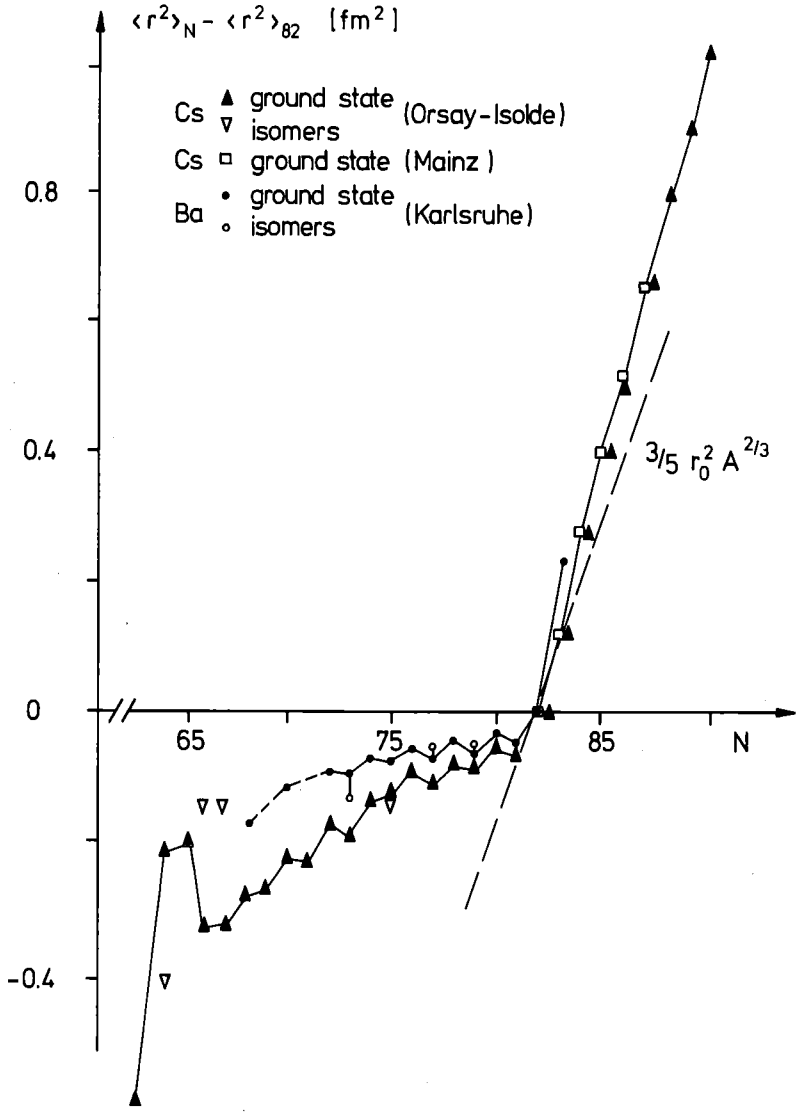

Fig. 18. Change of ms charge radii relative to N = 82*

The data include the ORSAY-ISOLDE results for neutron rich Cs isotopes produced by fission of uranium (Liberman et al. 1979)

long-lived isotopes of Ba, Cs and Xe (see Ullrich and Otten 1975). Similarily to the results of the Ba-measurements the data (fig. 18) seem to fit the assumption of gradually increasing nuclear deformation with decreasing neutron number. For very neutron deficient Cs isotopes ($N < 67$) the results exhibit very large fluctuations of $\delta\langle r^2\rangle$ as was observed in the Hg isotopes (see fig. 1). It should be noted that the uncertainty in the specific mass effect might considerably change the absolute scaling (up to 20 %) independently for each curve in fig. 18, but not the structure of the curves.

---

*Preliminary results for the neutron rich Ba isotopes (Mainz-Isolde collaboration): ^{139,140,141,142,143,144}Ba follow the line of the corresponding Cs isotopes fairly well (Mueller 1980).

5. Optical Isotope Shifts of Calcium Isotopes

The long isotopic chain between the two double magic nuclei ^{40}Ca and ^{48}Ca, where the neutron number changes by as much as 40 %, provides a unique play-ground for observing interesting nuclear structure effects in nuclear charge and matter distributions. The charge distribution of the stable nuclei has been extensively investigated by electron scattering, by muonic X-ray and optical isotope shift measurements. In recent time, there are also serious attempts in determining mass (and neutron) distributions by use of strongly interacting probes like pions, high energy protons and alpha-particles (Friedman et al. 1979). The only techniques which are able to extend our knowledge to the unstable Ca nuclei are laser spectroscopic observations of isotope shifts in optical lines (tab. 3). The Heidelberg group observed the extremely weak intercombination line (see fig. 19), which has the advantage of a rather small natural line width of 410 Hz.

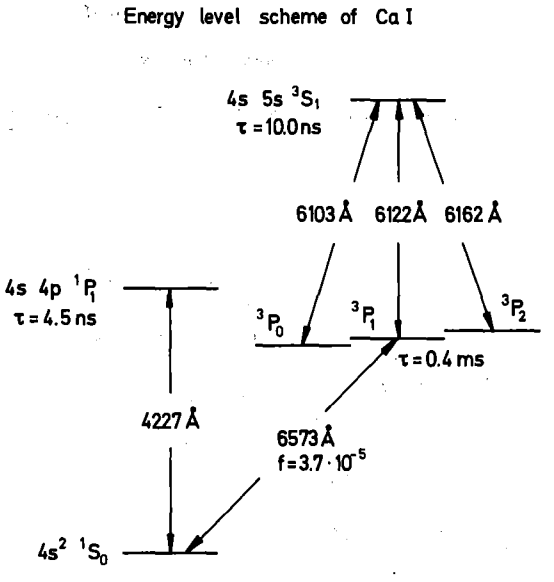

Fig. 19. CaI level scheme

The experimental technique applied by the HEIDELBERG group uses a collimated atomic beam and a stabilized dye laser which excites the different Ca isotopes by tuning the wave length. Due to the very long live time (τ = 0.4 ms) of the excited 4s4p $^3P_1$ level the whole beam emitts resonance fluorescence radiation along the

LASERSPECTROSCOPY OF THE CA-INTERCOMBINATION LINE

(HEIDELBERG GROUP)

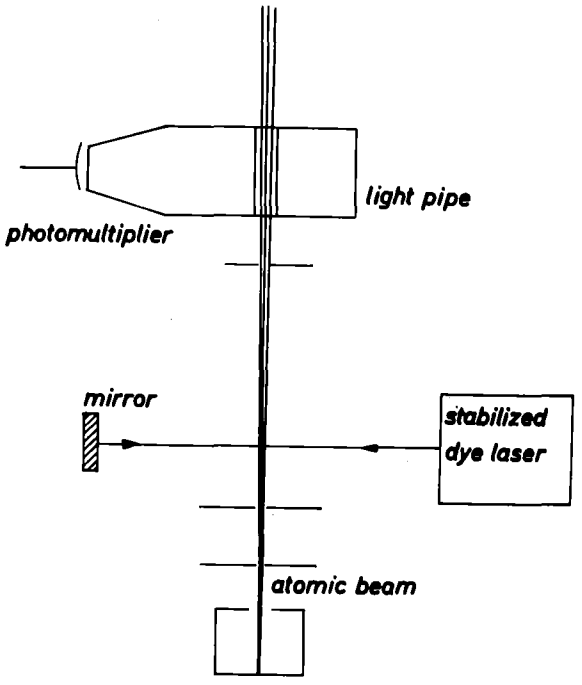

Scheme of the experimental set-up for laser-spectroscopy of the Ca-intercombination line

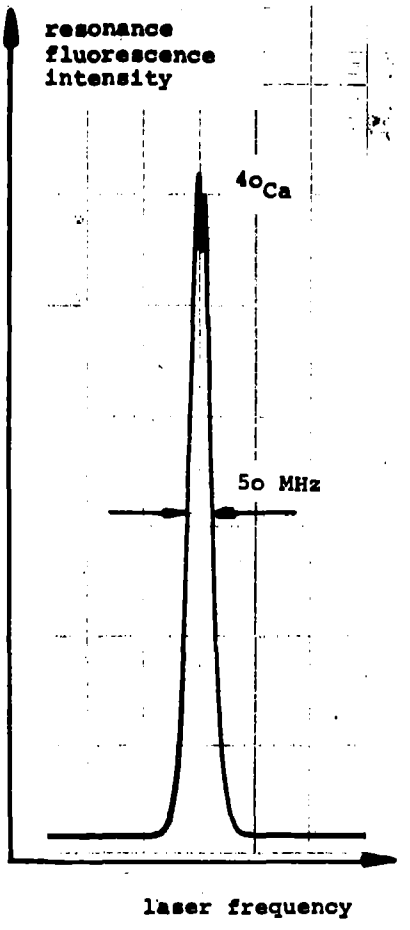

Lamb-dip in the Doppler profile

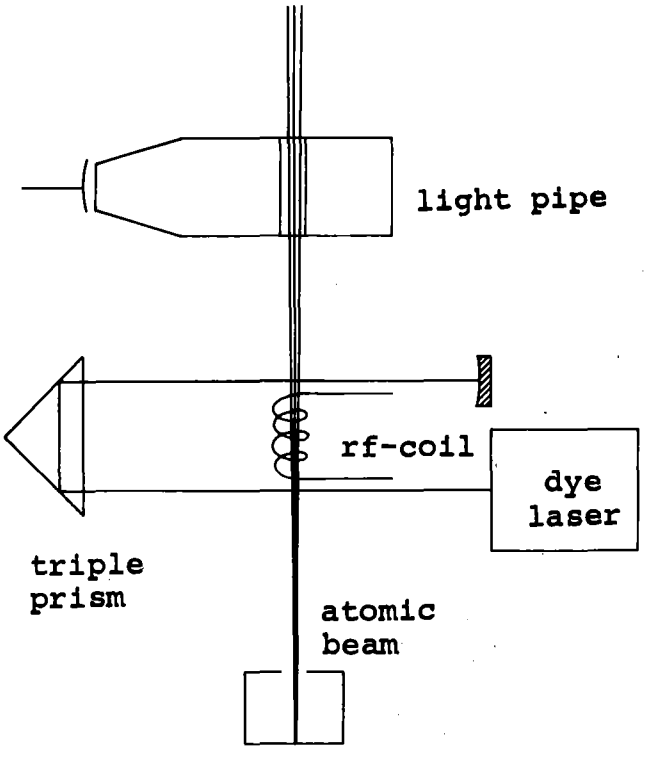

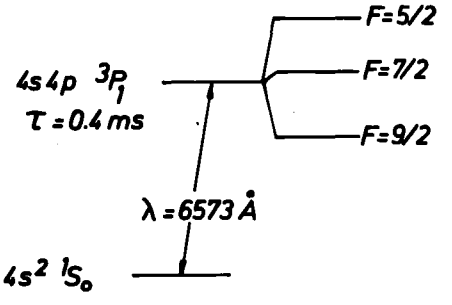

Detecting rf-transitions by saturated absorption

Fig. 20. Laserspectroscopy of the CaI intercombination line (Träger 1979)

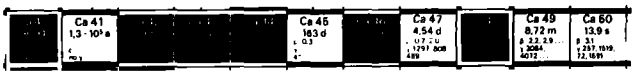

OPTICAL ISOTOPE SHIFT MEASUREMENTS IN CA

ANN PEREY (1959)		40-48	4227 Å (RESONANCE) 6103 Å 6122 Å 6162 Å CA^+-LINES	CONVENTIONAL OPTICAL SPECTROSCOPY
HEILIG (1968)		40-42-	RESONANCE LINE	
BRUCH ET AL. (1969)		44-48	CA^+-LINES	
EPSTEIN UND DAVIS (1970)		40-42 44-48	RESONANCE LINE	
BRANDT ET AL. (1977)	(1978)	40-42-43 44-46-48	RESONANCE LINE	
NEUMANN ET AL.(1976)		40-42-44- 46-48	INTERCOMBINATION LINE	LASER-SPECTROSCOPY
KLINGBEIL ET AL. (1979)		40-43		
KOWALSKI ET AL. (1979)		40-41		
BERGMANN ET AL. (1979)	(1980)	40-45 40-46		
ANDL ET AL.	(1980)	40-47	RESONANCE LINE	
BAIRD ET AL.	(1980)	40-48	1S - 2S TWO-PHOTON EXC.	

Tab. 3. IS-measurements in Ca-isotopes

path of flight of the atoms. Therefore the fluorescence can be monitored relatively far away from the excitation region which minimizes the (stray-)light background.
Though the isotope shifts are large as compared to the reduced Doppler-width of the atomic beam, the residual Doppler-broadening of about 50 MHz limits the resolution. Much narrower signals can be produced by simply reflecting the laser beam back onto itself. In this case so-called Lamb dips, free from Doppler broadening, can be observed at the center frequency of the Doppler profile, due to a saturation of the absorption. The counterprogating beam probes the bleaching of the sample when matching the center frequency. This technique (saturation spectroscopy) reduces the width of the signals of about a factor of 50.
For odd isotopes, where we find a hyperfine structure splitting the method has been combined with inducing radiofrequency transitions within the hfs, similar to the well known double resonance method, thus changing the occupation of the levels with refilling from the groundstate and increasing the emitted resonance fluorescence.

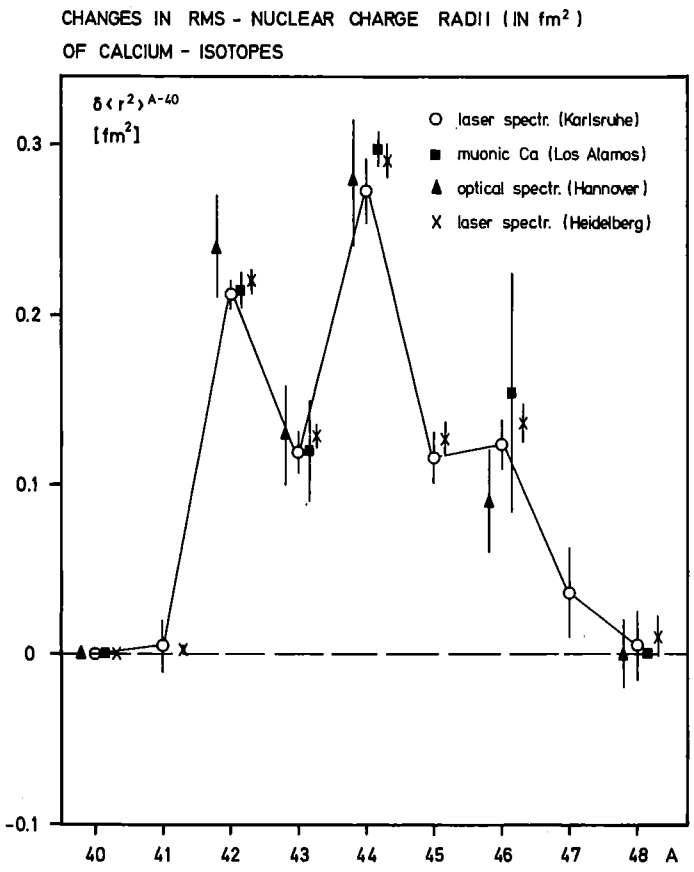

Fig. 21. Variation of rms charge radii in Ca isotopes

Fig. 21 compiles recent experimental results of optical isotope shift measurements of the CaI intercombination (Bergmann et al. 1980) and the blue resonance line (Andl et al. 1980), presenting rms radii differences and comparing with results of muonic X-ray studies (Wohlfahrt et al. 1978). Muonic X-ray shifts primarily are due to a different type of radial moments: Barret-radii. The conversion into equivalent rms-radii is not completely model-independent. A peculiar behaviour of the charge radii is obvious from fig. 21.

a. The charge rms-radii of ^{40}Ca and ^{48}Ca are equal whereas the even nuclei in between have a charge radius larger in size of about 1 %.

b. There is a considerable odd-even staggering. The odd ^{43}Ca nucleus is considerably smaller than the neighbours as far as the charge distribution is concerned.

The ^{47}Ca result - in that case the KARLSRUHE group recently succeeded exploiting the increased sensitivity when studying the resonance line - fits fairly well in the overall trend.

c. Within an error of 0.006 fm the radii of ^{41}Ca and ^{40}Ca are equal. This is interesting in view of the discussion of the ^{41}Ca - ^{41}Sc Coulomb-displacement energy, neutron excess radii and core compression effects (Friedman and Shlomo 1979).

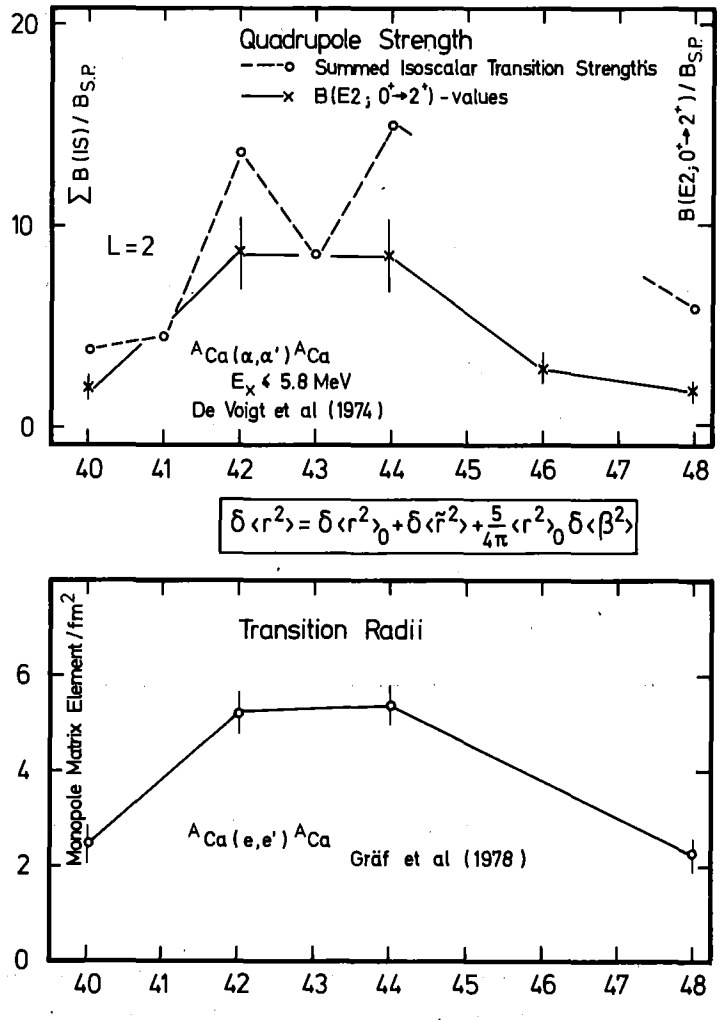

Fig. 22. Trends of proton, neutron and matter radii in the $f_{1/2}$-shell

The matter radii differences (extracted from alpha-particle scattering, e.g.) exhibit a different behaviour and rather closely follow the $A^{1/3}$ law, thus forming a neutron skin of ^{48}Ca (Gils et al. 1980).

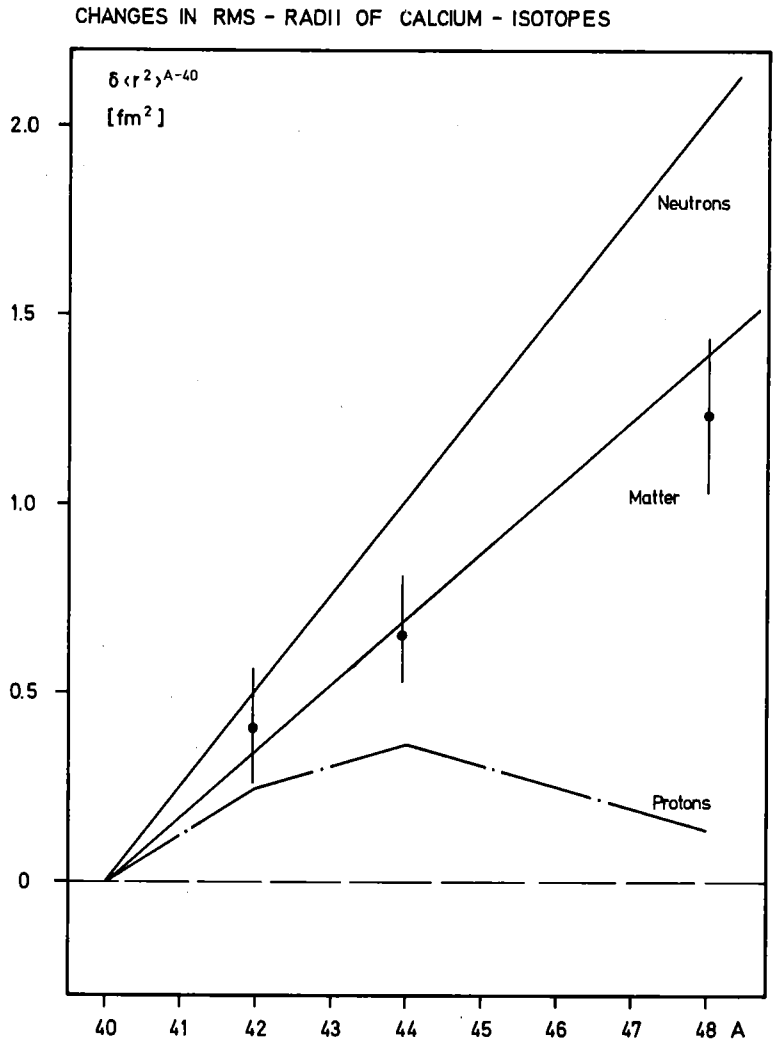

Fig. 23. Trends of the E2 strength and transition radii of Ca isotopes

Let us notice that there are conspicuously similar trends (fig. 23) in the quadrupole transition strengths inferred from inelastic alpha particle scattering (De Voigt et al. 1974), e.g. as well as in the transition radii measured for the $0_1^+ - 0_2^+$ monopole transitions by electron scattering by Gräf et al. 1978.
Again invoking the relation

$$\delta\langle r^2\rangle = \delta\langle r^2\rangle_o + \delta\langle \tilde{r}^2\rangle + \frac{5}{4\pi}\langle r^2\rangle_o \, \delta\langle\beta^2\rangle$$

with $\delta\langle r^2\rangle_o \equiv 0$ ($\langle r^2\rangle_o = \langle r^2\rangle_{^{40}Ca}$) the trend in $\delta\langle r^2\rangle$ may be fairly well ascribed to a deformation effect including a small breathing (monopole polarizibility) of the ^{40}Ca core.

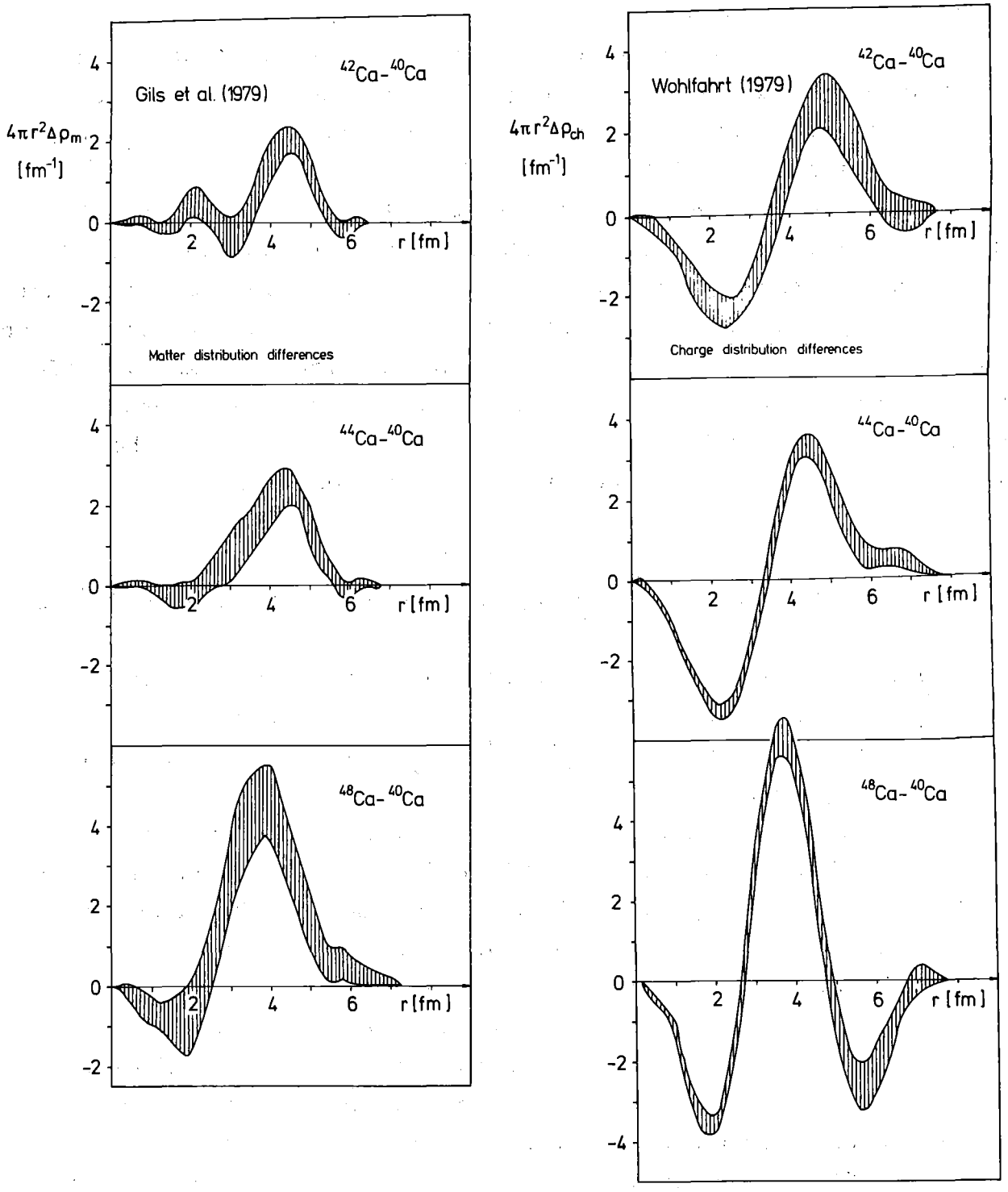

Fig. 24. Matter- and charge distribution differences in Ca nuclei

In Ca nuclei there is considerable evidence of a coexistance of strongly deformed core-excited configurations with $(fp)^n$ spherical configurations which mix in the low-lying states (Towsley et al. 1972). Fig. 24 is demonstrating the polarising interaction between the valence neutrons and the proton core. From extensive alpha particle scattering studies (Gils 1979, Gils et al. 1980) which inform us about matter distribution differences we know where the neutrons are localized (round the rms-radius of the $f_{7/2}$shell which is determined to be about 3.8 fm).
From corresponding electron scattering and muonic X-ray results (Wohlfahrt 1979) we see that obviously the neutrons have pulled the protons to the same place, in such an intriguing way that there is less charge at the ^{48}Ca surface than at the ^{40}Ca surface. Though equal in the rms charge radius, the distributions distincly differ. Recent theoretical approaches considering neutron and proton distributions of the Ca isotopes (Brown et al. 1979) have been remarkly successful in reproducing the observed findings.

6. Optical Isomer Shift of the Spomtaneous-Fission Isomer ^{240m}Am

The size and shape of a spontaneously fissioning isomer, the 1 ms ^{240m}Am, have been recently studied by measuring the optical isomer shift in the atomic $^8S_{7/2}$ - $^{10}P_{7/2}$ transition in neutral americium (Bemis et al. 1979).
The experimental technique: *Laser Induced Nuclear Polarization* (Feld and Murnick 1979) is a special application of the *Radiation Detected Optical Pumping* (see Jacquinot 1976). It is based on the depopulation by optical pumping with circularily polarized light. The optical pumping cycle consists of resonant absorption with the selection rule $\Delta M_F = +1$ for σ^+-light, followed by spontaneous radiactive decay with the selection rule $\Delta M_F = 0, \pm 1$. In absence of atomic ground-state relaxation, laser optical pumping with σ^+-light, with a band with greater than the total width of the $^{10}P_{7/2}$ hyperfine structure, ultimately results in the population of the ground-state level with $F_{max} = 7/2 + I$ and sublevel $M_F = + F_{max}$ from which no further laser absorptions may occur. The system both atomic and nuclear, is then totally polarized.

Subsequent spontaneous-fission decay from the oriented nuclear system is anisotropic, if $I \neq 0$ or 1/2, and the anisotropy of the decay provides the detection signal for the optical resonance condition.

Details of the experimental arrangement are given schematically in fig. 25. The isomer was produced by bombarding an uranium target with 48-MeV ^{7}Li ions. Fission isomeric recoils were thermalized in 180 Torr of heliumgas.

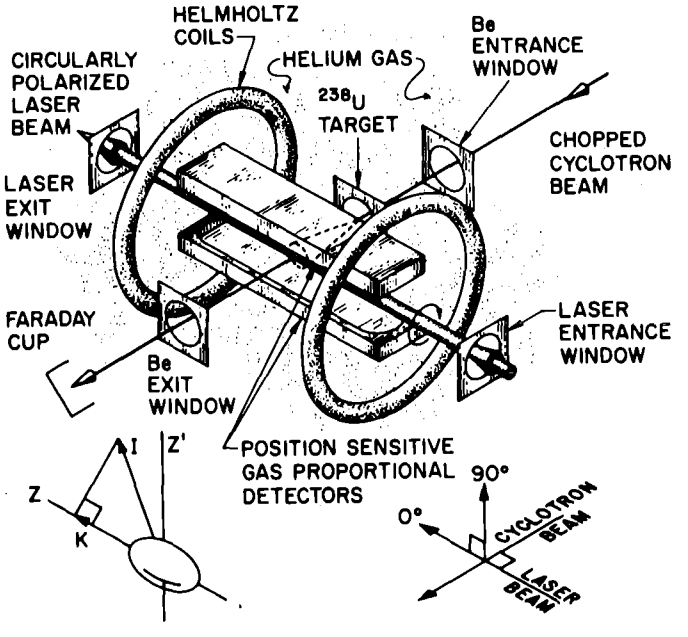

Schematic of the optical pumping cell showing the geometrical arrangement of the position-sensitive detectors, the laser beam, and cyclotron beam. The laser and cyclotron beams are both 0.4 cm in diameter.

Fig. 25. Schematic view of the experimental set-up used for measuring the optical shift in the lines of ^{241}Am and ^{240}Am (Bemis et al. 1979)

Two position sensitive detectors count the fission events. A small magnetic keeper field preserve the orientation of the atoms. Anisotropic decay from the oriented system with $K=I=M_I$ preferentially occurs along the laser beam propagation axis. Thus a decrease of the yield indicates the orientation produced by resonant optical pumping. This seems to be observed and appears

to be shifted by the unusually large value of $\Delta\lambda = 2.6$ Å against the known position of ^{241}Am (see fig. 26).

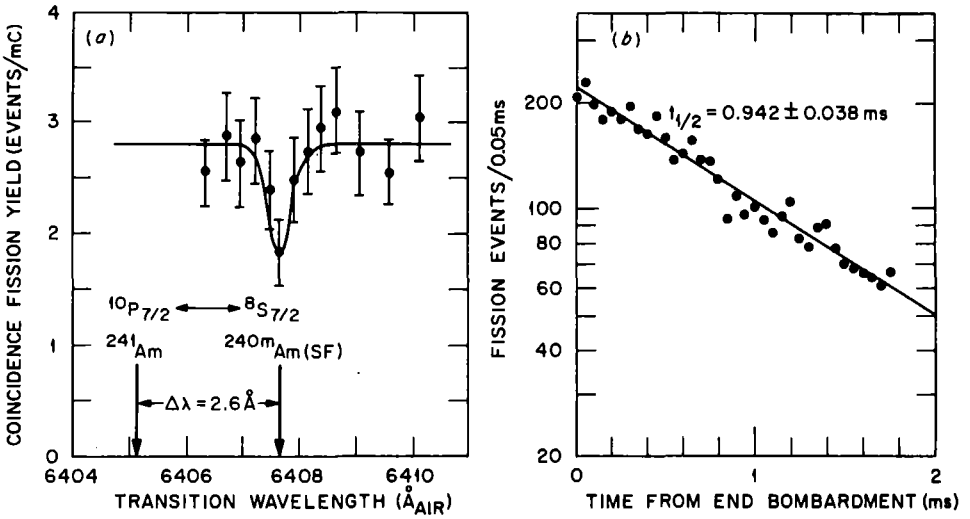

(a) Normalized fission-fragment coincidence yield as a function of laser wavelength. The decrease in yield at 6407.7 Å indicates anisotropic fission decay due to orientation via resonant optical pumping. The solid curve is shown to guide the eye. (b) The decay of fission events relative to the end of a beam-on cycle. The single-component decay is due to $^{240}Am^{m}(SF)$.

Fig. 26. Fission-fragment coincidence yield as function of the laser wave length and half-live control (Bemis et al. 1979)

From the observed isotope shift which is predominantly due to the volume effect a difference

$$\delta\langle r^2\rangle_{240m-241} = (26.8 \pm 2.0)\ \delta\langle r^2\rangle_{243-241}$$

is extracted, nearly independent of any nuclear and atomic model assumption. Clearly the result may point to a large deformation of the fission isomer ^{240m}Am.
Using the relation

$$\langle r^2\rangle = \langle r_o^2\rangle \left[1 + (5/4\pi)\ \langle\beta^2\rangle\right]$$

calculating the mean square radius of the charge distribution with the standard value $r_o = 1.2$ fm of the radius parameter and adopting $\beta = \langle\beta^2\rangle^{1/2} = 0.24$ from neighbouring Am isotopes the result has been converted into an isomeric shift

$$\delta\langle r^2\rangle_{240m-240g} = 5.1 \pm 0.2\ fm^2$$

The uncertainty allows for a normal odd-even staggering.
Again using the assumptions above a deformation of

$$\beta = 0.66$$

is found, and if assuming prolate, just describing a spheriod with a major-to minor axis ratio of 2:1.
There are considerable uncertainties in this argumentation. The monopole polarizibility ("isotope and isomeric shift anomaly") has been ignored. Therefore the deformation might be smaller than the value claimed. In addition the extracted $<\beta^2>^{1/2}$ is not a first order diagonal element (like a quadrupole moment). From this reason we can hardly follow the author's statement (Bemis et al. 1979) that their experiment provides the first direct experimental proof for large deformations. However, systematic high resolution experiments resolving hfs might be able to do so.

7. Concluding Remarks

This review tried to guide your interest to the experimental lines in atomic hyperfine structure and isotope shifts studies of unstable nuclei. With reference to recent examples we had an outlook to some laser spectroscopic techniques which enable the systematic study of long isotopic chains extending far off stability on proton-rich as well as on neutron-rich side. This special type of "nuclear spectroscopy" had already proven to be a rich source of relevant nuclear structure information, in particular when interacting with findings of nuclear gamma-ray spectroscopy, with the study of X-rays in ordinary and mesic atoms and with nuclear reaction experiments.

In many aspects this review is based on results and experiences from the experiments of the KARLSRUHE group (Bekk et al. 1979). It is a pleasure to acknowledge stimulating discussions with G. Nowicki and G. Schatz.

References

Andl A., Bekk K., Göring S., Hanser A., Nowicki G., Rebel H., and Schatz G. 1980 to be published - Contribution to "Trends in Nuclear Structure Physics" Manchester 16-18 April 1980

Anton K.-R., Kaufmann S.L., Klempt W., Moruzzi G., Neugart R., Otten E.W., and Schinzler 1978 Phys. Rev. Lett. 40 642

Arima A. and Iachello F. 1975 Phys. Rev. Lett. 35 1069

Arseniev D.A., Sobiczewski A., and Soloviev V.G. 1969 Nucl. Phys. A126 15

Baird P.E.G., Palmer Ch., and Stacey D.N. 1980 Private communications

Bauche J. and Champeau R.J. 1976 Advances in Atomic and Molecular Physics 12, 39 (ed. Bates D.R. and Bederson B., Academic Press New York - San Francisco - London)

Bemis C.E.Jr., Beene J.R., Young J.P., and Kramer S.D. 1979 Phys. Rev. Lett. 43 1854

Bekk K., Andl A., Göring S., Hanser A., Nowicki G., Rebel H., and Schatz G. 1979 Z. Physik A291 219

Bergmann E., Bopp P., Kowalski J., Träger F., and zu Putlitz G. 1979 Z. Physik A292 401

Bergmann E., Bopp P., Dorsch Ch., Kowalski J., and Träger F. 1980 Z. Physik A294 319

Bohr A. and Mottelson B.R. 1969 Nuclear Structure, Vol. 1 p. 163 (New York - Amsterdam: Benjamin Inc.)

Bodmer A.R. 1959 Nucl. Phys. 9 371

Bonn J., Huber G., Kluge H.-J., Kugler L., and Otten E.-W. 1972 Phys. Lett. 38 B 308

Bonn J., Huber G., Kluge H.-J., and Otten E.-W. 1976 Z. Physik A276 203

Bonn J., Klempt W., Neugart R., Otten E.-W., and Schinzler B. 1979 Z. Physik A289 227

Brandt H.-W., Heilig K., Knöckel M., and Steudel A. 1978 Z. Physik A288 241

Brown B.A., Massen S.E. and Hodgson P.E. 1979 Phys. Lett. 85 B 167 - J. Phys. G5 1655

Bruch R., Heilig K., Kaletta D., Steudel A., and Wendlandt D. 1969 J. Phys. (Paris) 30 suppl C1-51

Cappeler U. and Mazurkewitz W. 1973 Journ. of Magnetic Resonance 10 15

Cline and Flaum 1972 Proceed. Int. Conf. Nuclear Structure, Sensai, Japan (UR-NSRL-56)

Demtröder W. in Progress in Atomic Spectroscopy Part A 1979, eds. Hanle W. and Kleinpoppen H. (Plenum Press New York - London) p. 679

De Voigt M.J.A., Cline D., and Horoshko R.N. 1974 Phys. Rev. C10 1798

Epstein G.L. and Davis S.P. 1971 Phys. Rev. A4 464

Feld M.S. and Murnick D.E. 1979 in Laser Spectroscopy IV. Proceed. IV Internat. Conference, Rottach-Egern, Fed. Rep. of Germany June 11-15, 1979, eds. Walther H. and Rothe K.W. (Springer - Berlin - Heidelberg - New York) p. 549

Fischer W., Hartmann M., Hühnermann H., and Vogg H. 1974 Z. Physik 267 209

Friedman E. and Shlomo S. 1977 Z. Physik A283 67

Friedman E., Gils H.J., Rebel H., and Majka Z. 1978 Phys. Rev. Lett. 41 1220

Gerhardt H., Matthias E., Rinneberg H., Schneider F., Timmermann A., Wenz R., and West P.J. 1979 Z. Physik A292 7

Gerstenkorn S. 1979 Comments Atomic Mol. Phys. 9 1

Gils H.J. 1979 in: "What Do We Know about the Radial Shape of Nuclei in the Ca-Region?" Proceed. of the Karlsruhe International Discussion Meeting, May 2-4, 1979 KfK 2830 eds. Rebel H., Gils H.J., Schatz G. p. 123

Gils H.J., Friedman E., Majka Z., and Rebel H. 1980 KfK-Report 2839 - Phys. Rev. C. in press

Gräf H.D., Feldmeier H., Manakos P., Richter A., and Spamer E. 1978 Nucl. Phys. A295 319

Greenless G.W., Clark D.L., Kaufmann S.L., Lewis D.A., Tonn J.F., and Broadhurst J.M. 1977 Optics Comm. 23 236

Habs D., Klewe-Nebenius H., Wisshak K., Löhken R., Nowicki G., and Rebel H. 1974 Z. Physik 267 143

Hansen P.G. 1979 Ann. Rev. Nucl. Particle Sci. 29 69

Heilig K. 1968 Habilitation Thesis Hannover

Heilig K. and Steudel A. 1974 Atomic Data and Nuclear Data Tab. 14 C39

Höhle C., Hühnermann H., Meier Th., and Wagner H. 1978 Z. Physik A284 261

Huber G., Thibault C., Klapisch R., Duong H.T., Vialle J.L., Pinand J., Juncar P., and Jacquinot P. 1975 Phys. Rev. Lett. 39 332

Huber G., Bonn J., Kluge H.-J., and Otten E.-W. 1976 Z. Physik A276 187

Huber G., Touchard F., Büttgenbach S., Thibault C., Klapisch R., Duong H.T., Liberman S., Pinard J., Vialle J.-L., Juncar P., and Jacquinot P. 1978 Phys. Rev. C18 2342

Jacquinot P. in: High-Resolution Laser Spectroscopy - Topics in Applied Physics, Vol. 13, 1976, ed. Shimoda K. (Springer Berlin - Heidelberg - New York) p. 52

Kaufmann S.L. 1976 Optics Comm. 17 309

Köpf U., Besch H.J., Otten E.W., and von Platen C. 1971 Z. Physik 244 297

Klempt W., Bonn J., and Neugart R. 1979 Phys. Lett 82B 47

Kleinfeld A.M., Bockisch A., and Lieb K.P. 1977 Nucl. Phys. A252 526

Klingbeil U., Kowalski J., Träger F., Wiegemann H.-B., zu Putlitz G. 1979 Z. Physik A290 345

Kluge H.-J., Neugart R., and Otten E.-W., 1979, in: Laser Spectroscopy IV, eds. Walther H. and Rothe K.W. (Springer Berlin Heidelberg New York) p. 517

Kowalski J., Träger F., Weißhaar S., Wiegemann H.-B., zu Putlitz G. 1979 Z. Physik A290 345

Kühl T., Dabkiewicz P., Duke C., Fischer H., Kluge H.-J., Kremmling H., and Otten E.-W. 1977 Phys. Rev. Lett. 39 180

Kumar H. and Baranger M. 1967 Phys. Rev. Lett. 12 73

Liberman S., Pinard J., Duong H.T., Juncar P., Vialle J.L., Jacquinot P., Huber G., Touchard F., Büttgenbach S., Pesnelle A., Thibault C., and Klapisch R. 1978 CR Acad. Sci. Ser. B286 253

Liberman S., Pinard J., Duong H.T., Juncar P., Vialle J.L., Pillet P., Huber G., Touchard F., Büttgenbach S., Thibault C., Klapisch R., and Pesnelle A. 1979 in: Laser Spectroscopy IV, eds. Walther H. and Rothe K.W. (Springer Berlin Heidelberg New York) p. 527

Marshalek E., Person L.W., and Sheline R.K. 1963 Rev. Mod. Phys. 35 108

Meyer-ter-Vehn J. 1975 Nucl. Phys. A249 111, 141

Moskowitz P.A. and Lombardi M. 1973 Phys. Lett. B46 334

Mueller A.C. 1980 Private communication (Mainz-CERN-ISOLDE collaboration)

Myers W.D. and Swiatecki W.J. 1969 Ann. Phys. (N.Y.) 55 369

Myers W.D. 1969 Phys. Lett. 30B 451

Myers W.D. 1976 Atomic Data and Nuclear Data Tab. 17 411

Myers W.D. and Swiatecki W.J. 1980 Nucl. Phys. A336 267

Neumann R., Träger F., Kowalski J., zu Putlitz G. 1976 Z. Physik A279 249

Nowicki G., Bekk K., Göring S., Hanser A., Rebel H., and Schatz G. 1977 Phys. Rev. Lett., 332

Nowicki G., Bekk K., Göring S., Hanser A., Rebel H., Schatz G. 1978 Phys. Rev. C18 2369

Nowicki G. 1980 Private communication

Otten E.W. 1971 in: Hyperfine Interactions in Excited Nuclei, Vol. II. eds. Goldring V.G. and Kalish R. (Gordon and Breach Science Publ. New York - London - Paris) p. 363

Perey A 1954 Proc. Phys. Soc. A57 181

Puddu G., Scholten O., and Otsuka T. 1980 Preprint KVI 226 to be published

Reehal B.S. and Sorenson R.S. 1971 Nucl. Phys. A161 385

Rohoziński S.G., Dobaczewski J., Neslo-Pomorska B., Pomorski K., and Srebny J. 1976 Nucl. Phys. A292 66

Stacey D.N. 1966, Rep. Progr. Phys. 29 171

Schatz G. 1979 in: Laser Spectroscopy IV eds. Walther H. and Rothe K.W. (Springer Berlin Heidelberg New York) p. 534

Schinzler B., Klempt W., Kaufman S.L., Lochmann H., Moruzzi G., Neugart G., Otten E.-W., Bonn J., von Reisky L., Spath K.P.C., Steinacher J., and Weskott D. 1978 Phys. Lett. 79B 209

Sheline R.K., Sikkeland T., Chanda R.N. 1961 Phys. Rev. Lett. 7 446

Sternheimer R.M. 1950 Phys. Rev. 80 102 - 1967 Phys. Rev. 164 10

Stroke H.M., Blin-Stoyle R.J., and Jaccarino V. 1961 Phys. Rev. 123 1326

Träger F. 1979 in: "What Do We Know about the Radial Shape of Nuclei in the Ca-Region?" Proceed. of the Karlsruhe International Discussion Meeting, May 2-4, 1979 KfK 2830 eds. Rebel H., Gils H.J., Schatz G. p. 73

Towsley C.W., Cline D., and Horoshko R.N. 1972 Phys. Lett. 28 368

Ullrich S. and Otten E.-W. 1975 Nucl. Phys. A248 173

Vogg H. and Härtel R. 1977 Journ. Radioanal. Chem. 37 857

Wapstra A.M. and Bos H. 1977 Atomic Data and Nuclear Data Tab. 19 175

Wohlfahrt H. 1979 in: "What Do We Know about the Radial Shape of Nuclei in the Ca-Region?" Proceed. of the Karlsruhe International Discussion Meeting, May 2-4, 1979 KfK 2830 eds. Rebel H., Gils H.J., Schatz G. p. 57

Wohlfahrt H., Shera E., Hoehn M., Yamazaki Y., Fricke G., and Steffen R. 1978 Phys. Lett. 73B 131